



**LUND**  
UNIVERSITY

**Lunds Tekniska Högskola**

Department of Physics

# Diode laser frequency stabilization onto an optical cavity

---

Thesis work  
Master of Science in Photonics  
LRAP-473

Xingqiu Zhao

Supervisor:  
Ying Yan  
Lars Rippe

Lund 2013.03.25



## Abstract

During this thesis work, a frequency stabilization system for an External Cavity Diode Laser (ECDL) at 370 nm has been set up and tested. The goal of the frequency stabilization is to achieve a long term frequency stability of less than  $\pm 50$  kHz within 8 hours, which will be used for the single Ce ion detection project in the quantum information group.

The system design is centered around a Fabry-Pérot (FP) cavity which is composed of two mirrors optically contacted onto the ends of a cylindrical spacer made of Ultra-Low Expansion (ULE) glass. To first order, the cavity spacer has a zero thermal expansion coefficient around a certain temperature.

The method for achieving the required frequency stability is to actively stabilize the ECDL output frequency through controlling both the ECDL driving current and the grating position by a piezoelectric actuator. Pound-Drever-Hall (PDH) locking technique [1] is used to lock the laser frequency onto one of the resonance lines of the stable FP cavity. To be able to get the desired performance each segment of the system has to be set up correctly. The work include aligning the laser beam polarization, coupling laser into a single mode polarization maintaining fiber, setting up the radio frequency resonance tank used for the Electro-Optic Modulator (EOM), putting together the vacuum chamber where the FP cavity sits inside, installing the cavity spacer into the vacuum chamber, aligning the laser beam to match the cavity modes and designing the electronic filter circuits etc.

Finally, after eight months of hard work, this laser could be locked around 2 hours and gave a good start for the future work. However the locking performance has not been characterized due to the shortness of time. Considering the time plan for this thesis, the improvement for a longer-time locking is remained.

## Popular Science

The frequency stabilization technology plays an important role for precision measurement in many areas of science. In quantum computing field, the single ion detection also needs this technology for reading out a single qubit ion state.

In this master thesis, one 370 nm frequency stabilization system was set up and tested based on Pound-Drever-Hall technique. In this platform, the laser source is an External cavity diode laser, one piezoelectric transducer is attached onto the grating holder which changes the cavity length by using the voltage to control the piezoelectric transducer movement. Thus, there are two keys can stabilize the laser's frequency. One is the driver current adjustment and another one is the voltage control for the piezoelectric transducer displacement.

As the core of the stabilization platform, the Pound-Drever-Hall method can be simply explained like this: by using a Fabry-pérot cavity to measure the frequency of laser and an error signal can be detected when the laser is out of resonance with the cavity (the frequency of the laser was drifted). This error signal is analyzed by using the laser servo and then a correct signal will be sent to laser driver, the fine current adjustment stabilizes the laser's frequency. Figure 1 shows the basic layout of the Pound-Drever-Hall method. The solid and dash line corresponds to the light and electrical signal path, respectively.

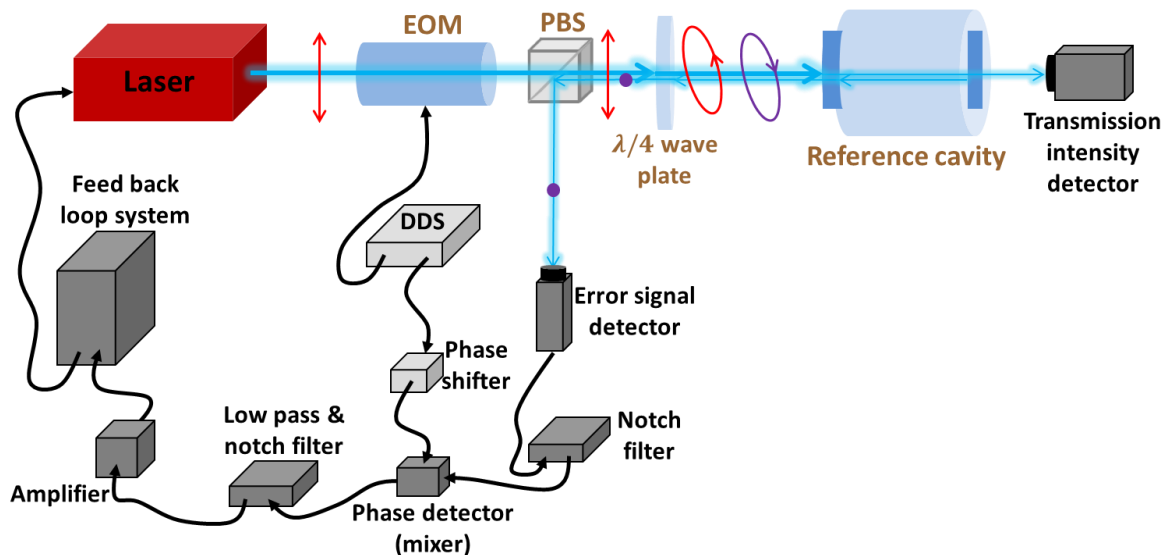


Figure 1. The basic principle diagram for PDH locking.

Finally, the frequency of the laser might be stabilized over few hours, but the actually result depends on the design target and testing process. For the correct error signal detection, there are many tasks should be solved one by one, such as the single mode polarization maintaining fiber coupling, electro-optic modulator alignment, mode matching with the cavity, electric device testing etc. Every segment might break the locking system, thus studying and recording the formation process of the stabilization system is necessary and valuable.

## **Abbreviations**

AC	Alternating Current
DC	Direct Current
DDS	Direct digital synthesizer
DP AOM	Double path acousto-optic modulator
ECDL	External cavity diode laser
EOM	Electro-optic modulator
FP cavity	Fabry-Pérot cavity
FSR	Free spectral range
LD	Laser diode
PBS	Polarization beam splitter
PDH	Pound-Drever-Hall
PM	Polarization maintaining
PZT	Piezoelectric transducer
TEC	Thermal electric cooler
RF	Radio frequency
ULE	Ultra-low expansion



## Contents

<b>Chapter 1 Introduction .....</b>	<b>1</b>
<b>Chapter 2 System Overview .....</b>	<b>3</b>
2.1 Sketch of the setup .....	3
2.2 External Cavity Diode Laser .....	6
2.2.1 Piezoelectric Transducer .....	6
2.2.2 Laser controller and servo .....	7
2.3 ULE cavity .....	9
2.3.1 Property .....	9
2.3.2 Vacuum chamber.....	11
2.3.3 Radiation shield.....	12
2.4 Introduction to Pound-Drever-Hall Locking.....	13
2.4.1 Working principle .....	13
2.4.2 EOM phase modulation.....	14
2.4.3 Error signal.....	15
<b>Chapter 3 Set up.....</b>	<b>16</b>
3.1 ECDL .....	16
3.2 Ultra Low Expansion cavity spacer .....	18
3.2.1 Bake out all components .....	18
3.2.2 The ULE cavity assembly .....	21
3.2.3 Pump the chamber to vacuum .....	25
3.3 PDH locking setup .....	27
3.3.1 Double Pass AOM.....	28
3.3.2 Single mode polarization maintaining fiber .....	29
3.3.3 Electro Optic Modulator.....	31

3.3.4 Electronic Filters .....	33
<b>Chapter 4 Test and Measurement .....</b>	<b>37</b>
4.1 Cavity mode matching .....	37
4.2 Error signal .....	39
4.3 Feed the error signal back to the laser servo .....	43
4.4 Future work .....	45
<b>Acknowledgments.....</b>	<b>46</b>
<b>Reference.....</b>	<b>47</b>
<b>Appendix .....</b>	<b>49</b>
Appendix A .....	49
Appendix B .....	52
Appendix C .....	54

## Chapter 1 Introduction

The motivation of stabilizing the laser frequency is to have a system which is able to detect a single Ce ion for the purpose of reading out a single qubit ion state. One of the important criteria in quantum computing is how to scale to large number of qubits. One way to construct multiple qubits is to let each ion represent one qubit, and then there is large possibility to find ion clusters which contains tens of ions for reasonable dopant concentrations [2]. However, in this approach the technique to read out a single qubit ion state needs to be developed. Wesenberg et.al suggested to add an additional ion (called as readout ion hereafter) into the same crystal as the qubit ions [3]. This readout ion has a strong interaction with the nearby qubit ion when they sit close enough to each other [4]. It will send out fluorescence photons when the qubit is at one level, otherwise not. A schematic diagram of the interaction is shown in Figure 1.1.

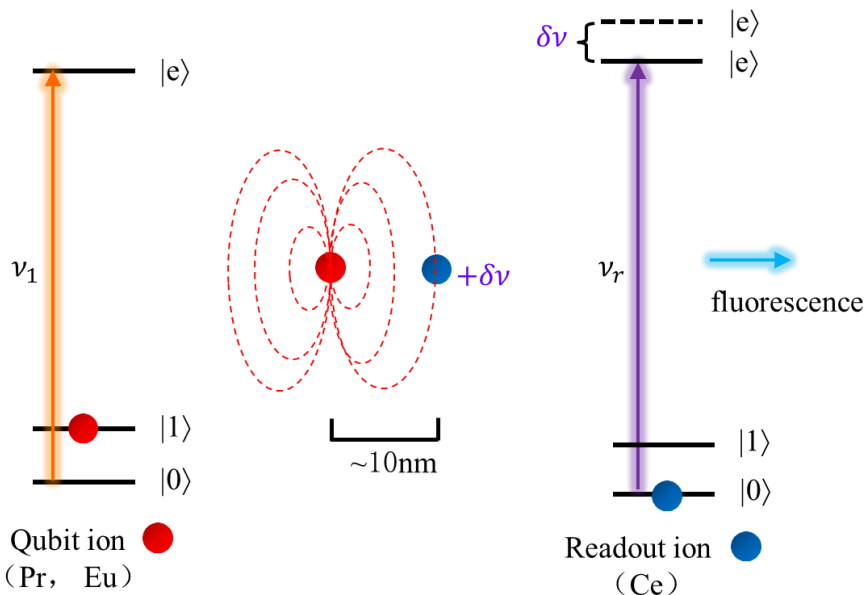


Figure 1.1. The readout ion schematic diagram [4]. The local E-field changes when the qubit ion is excited from  $|0\rangle$  to  $|e\rangle$  at frequency  $\nu_1$ , the transition frequency of the readout ion is changed with  $\delta\nu$ . So the frequency  $\nu_r$  cannot excite the readout ion anymore, and the fluorescence will be turned off.

This qubit state dependent fluorescence of the readout ion will help us to identify which state the single qubit ion is after the qubit operation is done. For doing that, we first need to develop a system capable of detecting a single readout ion by collecting its fluorescence. A stabilized laser is one part of that system. At this time, the Ce ion is considered as the candidate for as the readout ion. Because the excited state of Ce ion has lifetime of  $\sim 50$  ns and the transition linewidth is of  $\sim 3$  MHz. If we want the laser interacts with the same ion within a few hours and also want to keep a reasonable stable signal, then we would like the laser

frequency does not move 1/30 of the line width, which means the laser frequency should not drift more than  $\pm 50$  kHz over a few hours.

A laser diode can emit light over a range of a few nanometers and its output frequency depends on the injection current and the diode temperature strongly. To reduce the linewidth of a laser diode, an external cavity can be used [5]. However to obtain a stable and narrow linewidth frequency output, it is important to stabilize the diode's injection current and the temperature, also stabilize the length of the laser cavity. In the current external cavity diode laser the zero order beam reflects off the grating providing the output, while the first-order diffracted beam is directed back into the laser diode as a feedback. The optical feedback from the grating is spectrally narrowed and could be peaked at a frequency that differs from the central frequency of the free-running laser diode. The grating feedback narrows the laser linewidth down to  $\sim 1$  MHz [6]. To tune the central frequency of the laser, the tilt angle of the grating is adjusted by applying a voltage (0~150 V) to the Piezoelectric Transducer (PZT) attached on the grating holder.

For this project, the 370 nm laser frequency stabilization platform serves as the narrow linewidth laser source for detecting the single Ce ion, which is a key step for developing a scalable quantum computer hardware based on the rare earth ions [7].

This diploma work contains the following chapters:

Chapter 2 will introduce the components on the platform as well as the principle of the PDH locking scheme.

Chapter 3 emphasizes on the installation part of the vacuum chamber assembly and the components baking out procedures.

Chapter 4 is the testing process. The performance of the locking system have been recorded and discussed. Then is a short overview for the future work.

At the end of the report include 3 Appendixes:

(A) Two electronic filter design circuits.

(B) The cable connection diagram for the new laser controller.

(C) The baking data of the vacuum chamber recorded with some information note.

## Chapter 2 System Overview

This chapter will introduce the equipments used in the system and to some extent show the design idea behind the equipments. At the beginning of this chapter shows the outline of the platform. Next, the laser source and FP cavity will be introduced. Finally, the PDH locking principle will be presented in a simplified form.

### 2.1 Sketch of the setup

We wish the whole stabilization platform could be compact so that it can be easily moved to another lab in a nearby building, where the next experiment will run. For that purpose, an optical table with the size of 90 cm×70 cm was considered, which is right below the size of the door in most of the laboratories. However not sure we can fit all the components in such a limited area, so the first task of my thesis work is to make a real drawing of the whole system components to see if the platform is large enough. In this limited area, many components should be setup at the suitable and reasonable places. The flexibility and convenience of the light path should be considered. The design works were completed by using the Microsoft Visio. The final design is shown in Figure 2.1. This is a top view for the platform, all the components dimension (top view) should be set correctly at first. The next step is to arrange the position of the components, the laser beam should not be blocked and overlapped. In some special cases, the beam height will be changed, e.g. the DP AOM and the error signal detection path. The dashed and dotted line in Figure 2.1 indicates these two parts, respectively. Moreover, some adjustments need to be done when we do the testing, so the distances between each component should be considered, e.g. DP AOM, Electro-optic modulator (EOM) alignment, fiber coupling, mode matching, etc. The mode numbers and manufacturers of all components are listed in Table 1.

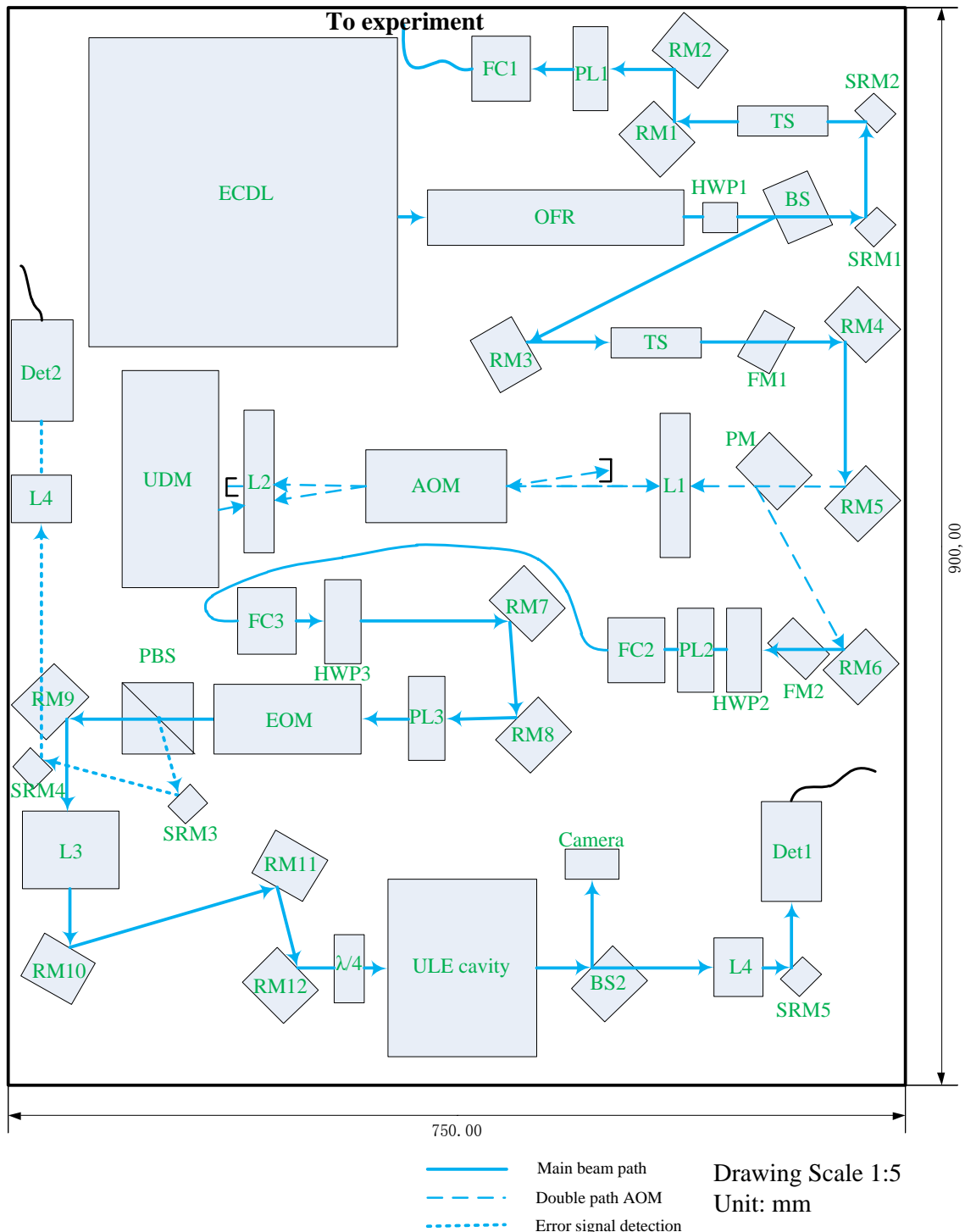


Figure 2.1. Overview of the optical components on the platform. About the detail components information please see Table 1.

Table 1. List of the components on 370nm stabilization platform

Code in Figure 6	Component	Model	Manufacturer
ECDL	External cavity diode laser	-	Home made
OFR	Optical faraday rotator	IO-5-370.7-HP P/N	Thorlabs
HWP	Half wave plate	WPZ-1310-370-L/2	CASIX
BS1	Beam splitter	BSS10	Thorlabs
RM1~12	Dielectric mirror Ø1"	BB1-E01	Thorlabs
SRM1~5	Dielectric mirror Ø1/2"	BB05-E01	Thorlabs
PM1~2	Pick up mirror	BB1-E01	Thorlabs
L1, L2	Plano-convex lens	LA1979-A	Thorlabs
UDM	Up and down mirrors	BB1-E01	Thorlabs
FM1~2	Flip mirrors	BB1-E01	Thorlabs
PL1~3	Polarizers	GLP6306	Foctek
FC1~3	Fiber coupler	KT110	Thorlabs
	Adaptor for fiber coupler	19.5AM 25	Schafter Kirchoff
	Polarization maintaining fiber	PM-S350-HP	Thorlabs
	Fiber adapter plate	SM1FCA	Thorlabs
PBS	Polarization beam splitter cubes	custom order	Foctek
L3	Plano-convex lens	LA1172-A	Thorlabs
$\lambda/4$	Quarter wave plate	custom order	CASIX
ULE cavity	ULE spacer	custom order	Advanced Thin Film
	Vacuum chamber	SPE-10028975-10-1	Vacom
BS2	Beam splitter	BSS10	Thorlabs
Camera	Camera after ULE cavity	FFMV-03M2M-CS	Point Grey
D1	Transmission intensity detector	HCA-10M-100K-C	Femto
D2	Error signal detector	HCA-S	Femto
AOM	Acoustic-optic modulator	1250C-829A	ISOMET
EOM	Electro-optic modulator	PM25 KD*P	Linos

## 2.2 External Cavity Diode Laser

The line center of the Ce ion (in an  $\text{Y}_2\text{SO}_5$  crystal) transition is at 370.7 nm (air wavelength). The laser source selection is the first step. Laser Diode (LD) is a very popular laser source and there are diodes emission covering this wavelength. Comparing with other laser source, the LD has many advantages such as small volume, light weight, convenient modulation, quake-proof and so on. But a LD is very sensitive to overhead driving current and static electric shots. A good illustration of the ECDL working principle can be found in Chapter 3 of the reference [5]. The cavity length of the ECDL is about 2 cm and the corresponding Free Spectral Range (FSR)  $\Delta f_{FSR}$  is

$$\Delta f_{FSR} = \frac{c}{2nL} = 7.5 \text{ GHz}$$

where  $n$  is the refractive index of air,  $L$  is the cavity length.

Figure 2.2 shows the ECDL inside structure. The positions of the main components are shown in the left panel of the figure.

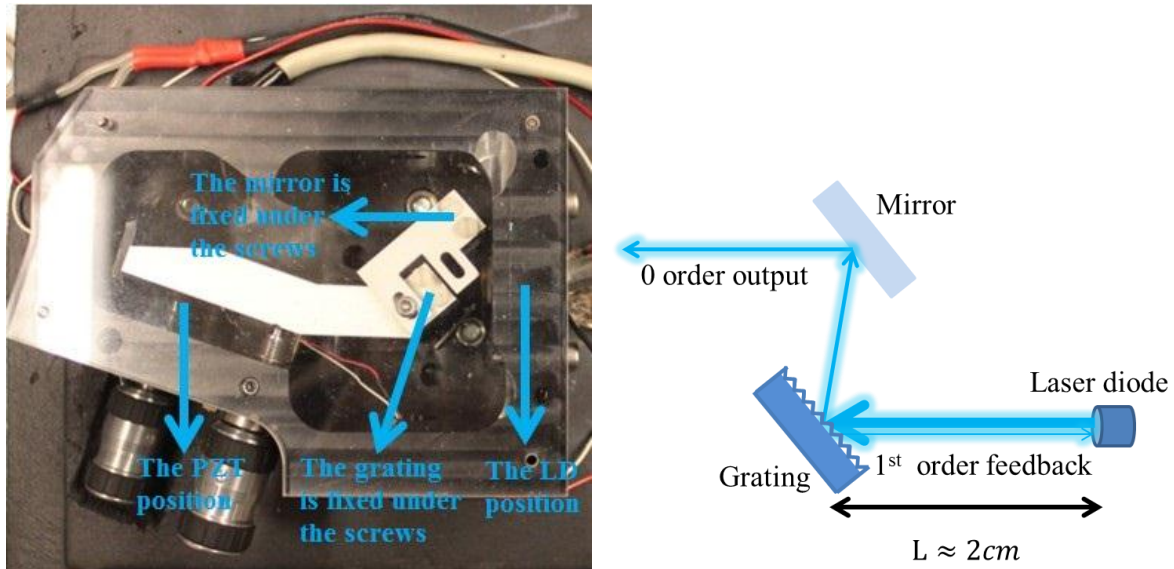


Figure 2.2. The structure of the ECDL

### 2.2.1 Piezoelectric Transducer

Changing the cavity length is a necessary step to scan the laser frequency. PZT can be used to change the cavity length when it is attached to one of the cavity optics, as an example here the PZT is attached to the grating holder and the position is shown in Figure 2.2. By controlling the supply voltage to PZT its physical length can be changed due to the electrostriction effect. The maximum range of its length can change is a property of the material.

Considering a thermal expansion coefficient of the aluminum (grating holder  $22.2 \times 10^{-6}$  m/m K), the laser cavity length variation over  $\pm 5$  °C is 0.94 um. To compensate for this thermal drift, one small PZT was ordered from Thorlab and the supply voltage is from 0~150 V (apply positive voltage to upper limit, reverse bias will destroy the PZT) corresponding to a length deformation of 0~4.6 um. Considering the angle between the normal line of the grating surface to the incident laser beam, 4.6 um displacement roughly corresponds to a cavity length change of 1.38 um. The change of the laser frequency ( $\delta f$ ) relates to the cavity length change ( $\delta L$ ) as

$$\delta f = \delta L \times \frac{\Delta f_{FSR}}{\lambda/2}$$

Where  $\Delta f_{FSR}$  is the FSR of the laser cavity, and  $\lambda$  is the wavelength of the laser. So the maximum frequency change which the PZT can compensate is about 50GHz.

The dimension of the PZT is shown in Figure 2.3. In ECDL the piezo was installed on the grating holder, and the position is shown in Figure 2.2. One thing is worth to be noted for the PZT installation, to prevent the PZT from being destroyed by the directly contact of the strong (hard) screw tip, one sapphire disk was glued on the end of the PZT.

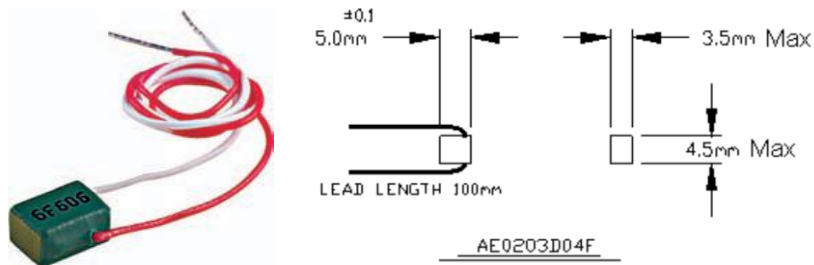


Figure 2.3. The PZT drawing

## 2.2.2 Laser controller and servo

The laser controller and servo were manufactured by Vescent Photonics. The laser controller supplies the driven current to laser diode and the servo receives the error signal meanwhile output two signals. One is the error correction signal to laser driving current. The other is the correction signal to PZT voltage. They share one power supply. Figure 2.4 shows a photo of them.

The laser controller contains two temperature controllers and a 200 mA diode laser driver based on the Libbrecht-Hall circuit [8]. One temperature controller controls the temperature of the laser house, the other controls the temperature of the LD, both of them setting range is 1~50 °C and the long term stability is around 1 mK/day. The current noise density is lower than  $100 \text{ pA}/\sqrt{\text{Hz}}$ . This is one of the fewer laser diode drivers with such low current noise on the market, which is very important for the frequency stabilization. The extremely fast current

modulation type is designed for the laser controller which can process the high-speed signal from servo control to adjust the laser's frequency. The current servo input matches with the  $1\text{ k}\Omega$  impedance and supports input frequencies up to 10 MHz.

The Laser Servo contains a tunable PI<sup>2</sup>D loop filter for firm locking to an error signal. It can work either in side lock mode or in peak lock mode. These two modes were described in [8]. In our system, the peak lock mode has been chosen because we want to lock the laser frequency onto the peak position of the resonance line of the FP cavity. In this mode, the user can select the zero-crossing by add a Direct Current (DC) offset to the error signal if one wants to lock the laser at an offset frequency relative to the resonance line. The slope of error signal can be either positive or negative, one switch controlling this is on the front panel. The input and output impedance is  $50\ \Omega$  and the maximum input voltage signal amplitude from -500 mV to +500 mV. Additionally, there is an internal ramp generator included. It could be used to sweep the PZT voltage. The amplitude of the sweep is from -5 V to +5 V in dipolar mode and the frequency is 500 Hz. However the supply voltage to PZT has to be positive otherwise the PZT possibly be permanently destroyed. One way to solve that problem is adding a voltage offset to the auxiliary output from the laser servo before the signal goes to the PZT as shown in [Section 4.3](#).

More information on the laser servo and controller can be found on the home page: [www.vescentphotonics.com](http://www.vescentphotonics.com)

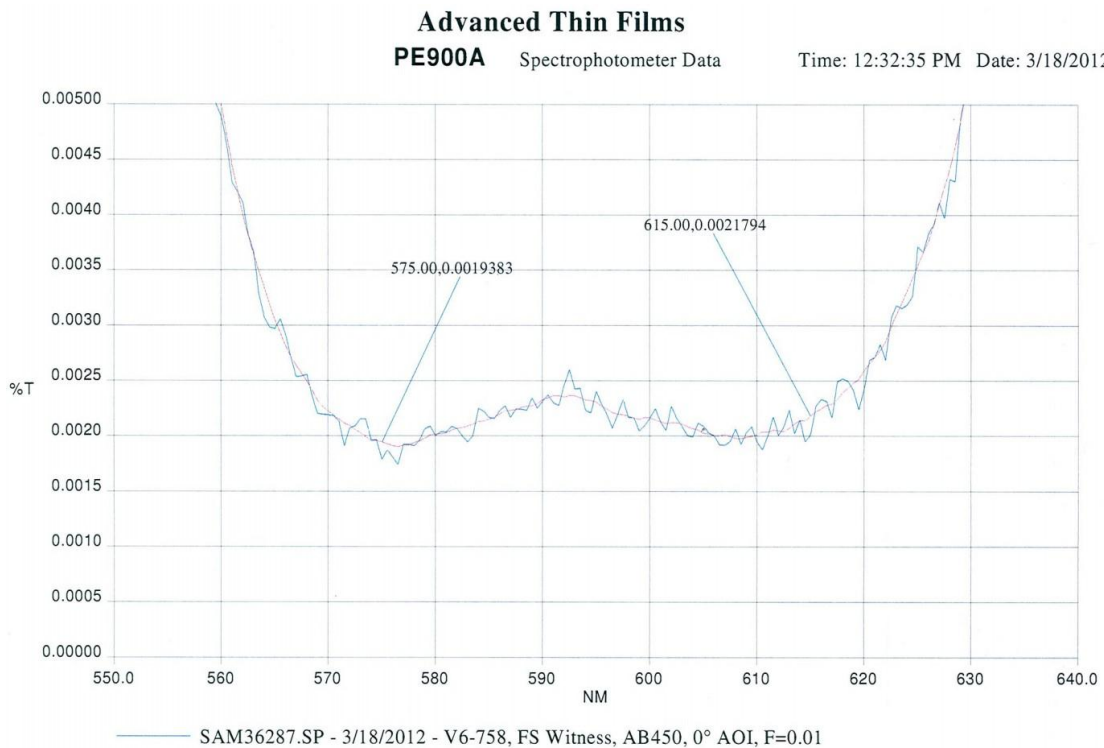


Figure 2.4. The laser control system

## 2.3 ULE cavity

### 2.3.1 Property

The FP cavity which is made of premium grade ULE glass is the essential part of the whole system. The ULE glass has a very low thermal expansion coefficient ( $0 \pm 30 \times 10^{-9} \text{ m/m} \cdot \text{C}$ ) at zero crossing temperature [9] and the length of the cavity won't change with the temperature to the first order around its zero crossing temperature. In our system, the cavity was ordered from [Advanced Thin Film company](#). This is a cylindrical cavity with diameter of 44 mm and the length of 55 mm, a 6 mm diameter hole along the cylindrical axis permitting the laser beam pass through, and two sink holes on each side for the supporting purpose [10]. The reflectivity of the mirror coating is shown in Figure 2.5. It is a high reflectivity coating covering two bands of 575-615 nm and 365-375 nm.



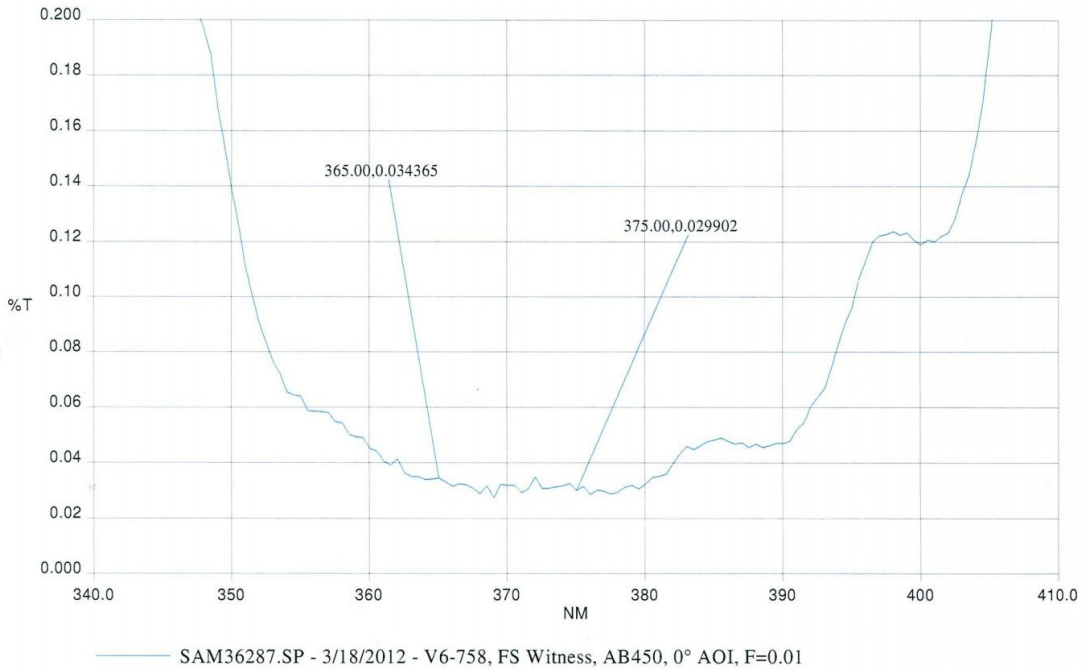


Figure 2.5. The reflectivity of the cavity mirror coating

The basic parameters of this cavity are as following.

The FSR is

$$\Delta\nu = \frac{c}{2L} = 2.7\text{GHz}$$

Cavity finesse is

$$F \approx \frac{\pi\sqrt{R}}{1-R} = 30000$$

where  $c$  is the speed of the light,  $R$  is the mirror reflectivity of 99.99% (seen from Figure 2.5) around 370 nm.

The line width

$$\delta\nu = \frac{\Delta\nu}{F} = 90\text{ kHz}$$

The cavity mirrors were also made of premium grade ULE, optically contacted to each end of the cavity spacer. Figure 2.6 shows this cavity. The two mirrors have the same high reflection coating and the parameters shows in Figure 2.5. However the coating areas are different, the larger one is on the concave mirror and the small one is on the plane mirror. To identify these two mirrors is very important for the later cavity mode matching which will be introduced in [Section 4.1](#).

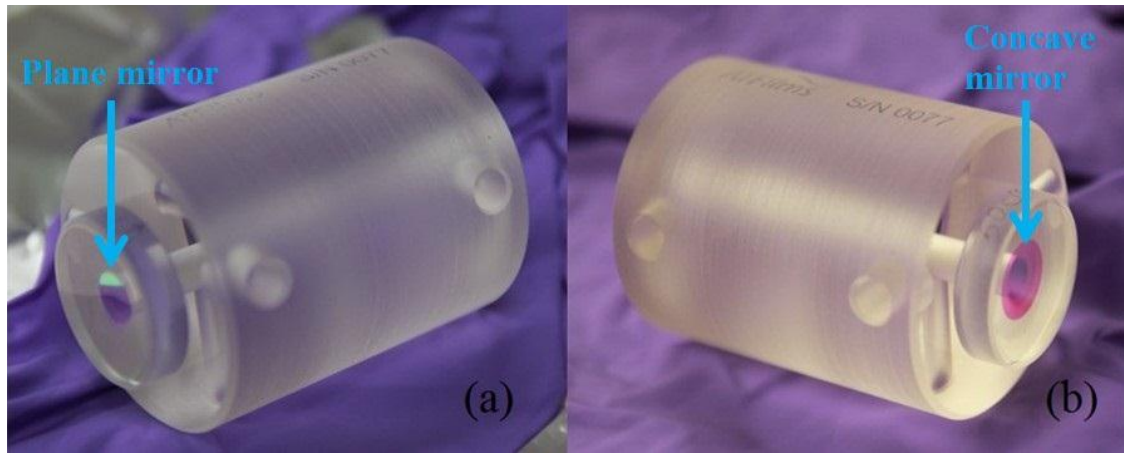


Figure 2.6. The ULE cavity

### 2.3.2 Vacuum chamber

A vacuum chamber is needed for ULE cavity, because the disturbance caused by the thermal convection, acoustic and pressure vibration will be minimized. Since the system is limited by space, one mini vacuum chamber is designed by Ying Yan and custom ordered in Vacom. Figure 2.7 shows this mini vacuum chamber with a length of 120 mm. The port A is for connecting to a turbo pump, port B is for the connection to an ion pump port and port C (on the opposite side of port B) is for the electric feed through for the Thermal Electric Cooler (TEC) inside the cavity. The installation details will be shown in section 3.2.



Figure 2.7. The vacuum chamber

### 2.3.3 Radiation shield

The radiation shield supplies a shielded and constant temperature environment. The material of the radiation shield is copper which has good thermal conductivity, thus the uniform temperature can be provided inside the radiation shield. The gold coating reflects most of incoming thermal radiation back and keeps the ULE cavity less disturbed by the outer environmental temperature. Figure 2.8 shows the radiation shield. Part A shows the threaded M3 (1.6 mm) holes where a screw will be fit in for the purpose of supporting the ULE cavity spacer. The detail connection will be introduced in Chapter3. Part B is the lid for radiation shield and in the middle of the lid there is a window (part C) for light path and the transmission efficiency of the window coating is larger than 99.9% @ 370 nm. Part D shows the venting holes for the pumping purpose. Those holes should have a proper lean angle. On one hand should keep the ventilation air path short so that not decreasing the pump speed much. On the other hand the radiation flowing along the hole should not hit the cavity spacer for the purpose of minimizing the thermal radiation influence on the cavity temperature variation. The two lids will be mounted onto the cylinder structure by M3 (1.6 mm) screws. It is important to note that all screws used in vacuum chamber must have vented holes along its axis, otherwise the air could be easily trapped inside and it will be a problem to achieve a higher vacuum level.

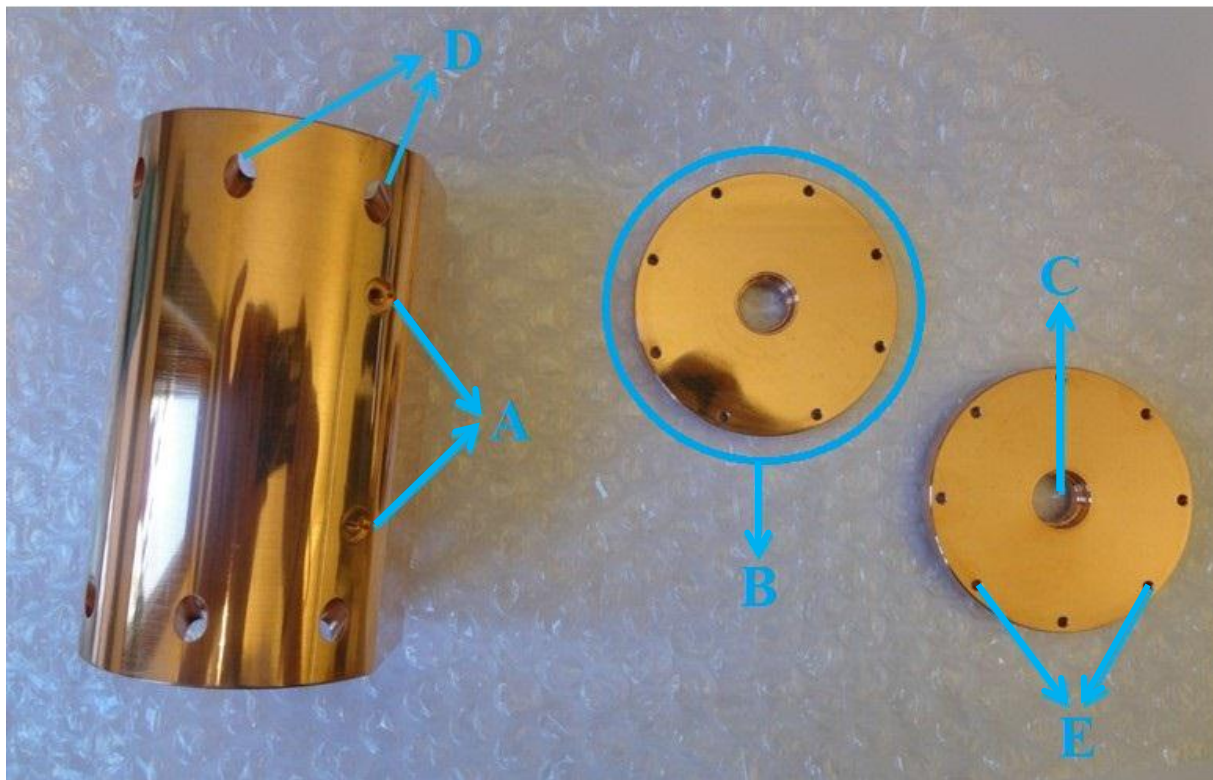


Figure 2.8. The radiation shield

## 2.4 Introduction to Pound-Drever-Hall Locking

### 2.4.1 Working principle

The essential part of the PDH locking is doing a phase modulation on the input light so that the beam contains a carrier frequency and two sidebands. The phase modulation will be introduced in next section. The reflected beams can be seen as the coherent superposition of two fields. One is the direct reflection from the first mirror of the cavity and another one is the leakage field from the intra cavity field. These two fields are  $180^\circ$  out of phase, when the incoming light is on resonance with the lossless ULE cavity. In this case these two fields will cancel each other completely. Otherwise, there is a non-zero residual field left from the interference of these two fields. This residual field contains the error signal information.

Figure 2.9 shows the basic diagram for a PDH locking. The solid and dash line corresponds to the light and electrical signal path, respectively. In order to separate the incoming light and the reflected light, one Polarization Beam Splitter (PBS) cube and a  $\lambda/4$  plate is set before the cavity. The polarization state of incoming light should be in pure linear (vertical or horizontal), thus the reflected light will be rotated  $90^\circ$  compare with the incoming light. In this approach, the reflected light can be picked with the PBS cube.

The error signal is created from a mixer, where the signal from the error signal detector multiplied with a signal from the DDS. Then the signal passes through one phase shifter and two filters (one is low pass filter and another one is the low pass & notch filter). According to the error signal the laser controller will adjust the driver current on a time scale of  $\mu\text{s}$  and the voltage to the PZT on a slower time scale of ms, both of them keep the laser working on resonance with the cavity, thus the laser frequency is stabilized [1].

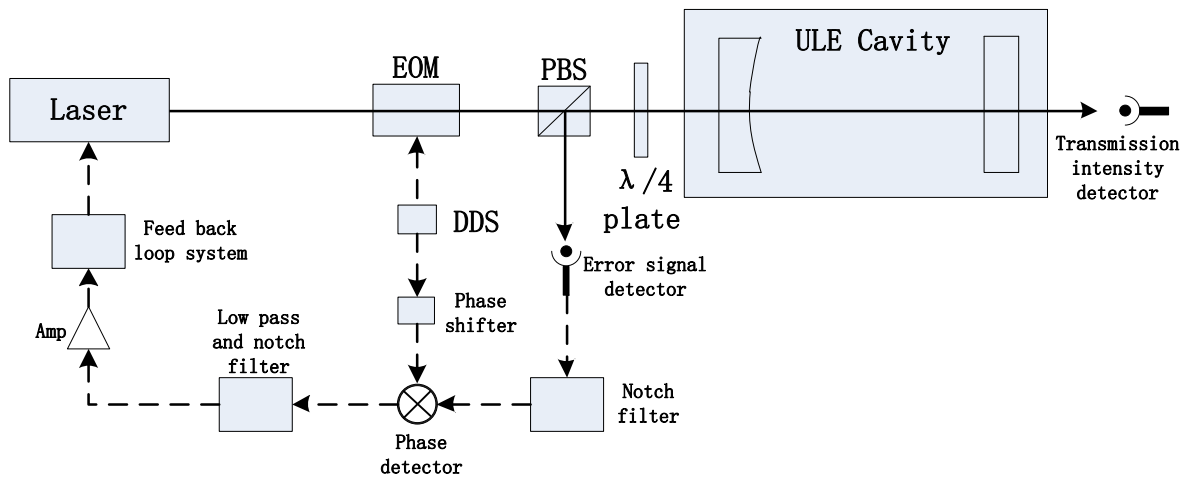


Figure 2.9. The basic principle diagram for PDH locking.

## 2.4.2 EOM phase modulation

As mentioned in previous section, the laser beam should be phase modulated before going to the ULE cavity. An EOM can do the job. It is a device based on the electro-optical effect, the crystal changes its reflective index when an electric field is applied. The electric field of the light passed through the EOM has the following expression,

$$E = E_0 e^{i[\omega_0 t + m \sin(\omega_m t)]}$$

where  $E_0$  is the amplitude of the incoming E-field,  $\omega_0$  is the frequency of the incoming light,  $\omega_m$  is the modulation frequency, and the  $m$  is called as modulation index which is the effective amplitude of the modulating field. If the modulation index is small, the equation can be written as

$$\begin{aligned} E &= E_0 e^{i[\omega_0 t + m \sin(\omega_m t)]} \\ &\approx E_0 [J_0(m) e^{i\omega_0 t} + J_1(m) e^{i(\omega_0 + \omega_m)t} - J_1(m) e^{i(\omega_0 - \omega_m)t}] \end{aligned}$$

These three parts corresponds three different frequencies. The first one is the carrier frequency, and the other two are the sidebands with plus and minus the modulation frequency offset relative to the carrier [11]. The Radio Frequency (RF) source used for the EOM phase modulation needs to have a low phase noise and good frequency stability. A Direct Digital Synthesizer (DDS) (Model 409B from Novatech) was used, with low enough phase noise and high frequency stability. This DDS has four independent output channels for sinusoidal wave with maximum output of 1 V<sub>pp</sub> into 50 ohm. The frequency range is from 0.1 Hz to 171 MHz and the step is 0.1 Hz. The RF signal power is too low to achieve the required modulation index ( $m = 1.08$  is an optimal modulation depth [1]), so one high power amplifier (ZHL-20W-13+, Minicircuits) was used. The amplifier has a gain of ~50 dB (slightly varies for different RF frequencies and with different supply voltage). In order to decrease noise contribution from the supply voltage, A linear power supply was selected. The linear power supply generally has much low noise than a switched-mode power [12].

Even with the amplification of the above mentioned amplifier, the peak to peak supplying voltage of the RF signal is only 5.9 V. However, according to the datasheet of the EOM, the  $\lambda/10$  voltage at 633nm is 200V. It relates the EOM material parameters as

$$V_\pi = \lambda \cdot \frac{d}{n_e^3 r_{33} \cdot l}$$

where,  $V_\pi$  is known as the half-wave voltage. It is the applied voltage at which the phase shift changes by  $\pi$ .  $d$  is the thickness of EOM crystal,  $l$  is the length,  $n_e$  is the refractive index of the EOM, and  $r_{33}$  is element of EOM tensor. From this the half wave voltage at 370 nm is calculated as 585 V and for achieving a modulation index of 1.08, 402 V peak to peak voltage is required.

In order to achieve this, the resonance tank is used. A simple LC resonance circuit is contained in the resonance tank, Figure 2.10 shows the structure of the homemade resonance tank and the simple electronic diagram is on the right. The circuit was designed and tested by Mahmood (PhD student in the quantum information group).

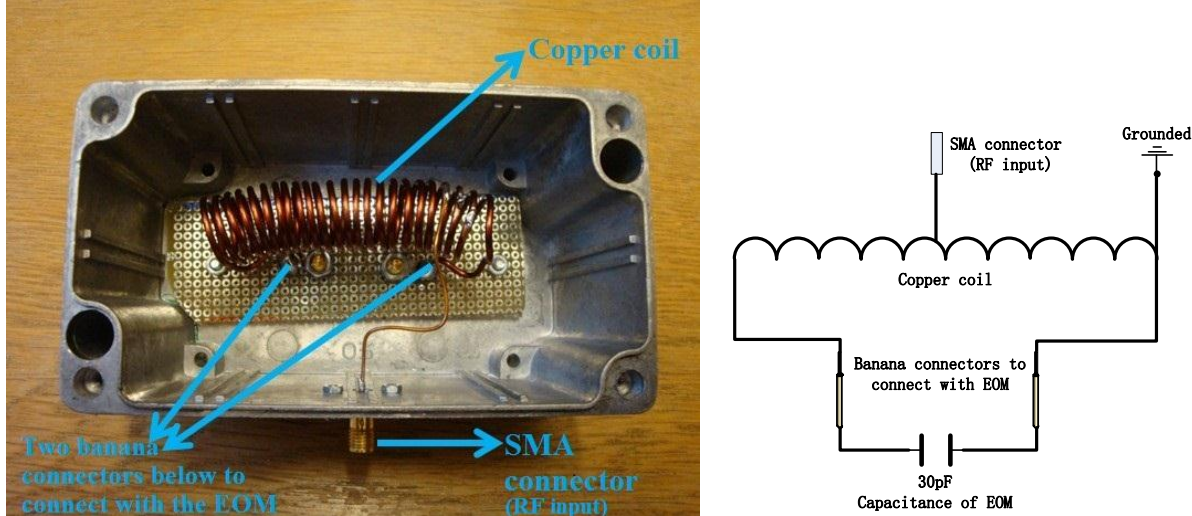


Figure 2.10. The resonance tank for 370nm stabilization system.

#### 2.4.3 Error signal

As mentioned in previous section, the electric field of the incoming light contains three different frequencies. For the carrier, the frequency error can be detected when the incoming light is out of resonance with the cavity, in order to know the polarity of the frequency error, a phase modulation is done before the cavity. A very good illustration about how the sidebands help to identify the error polarity in terms of field interference is shown in [11].

When the incoming light is on resonance with the cavity, the two sidebands beat with each other generating a  $2 \omega_m$  intensity modulation on the reflected beam; otherwise, the reflected signal has a beat pattern at frequency of  $\omega_m$ . The reflected signal is an Alternating Current (AC) signal which is detected by a high-speed photodetector HCA-S (custom made by Femto). This signal multiplies with a synchronized sine signal which with the same frequency as the phase modulation via a phase detector (mixer), so the output of the mixer contain signal both DC term and AC term with twice modulation frequency. Here the low frequency signal is the useful part. One low pass filter on the output of the mixer extracted this low frequency signal which is called as error signal. The recorded error signal will be shown in [Section 4.2](#).

## Chapter 3 Set up

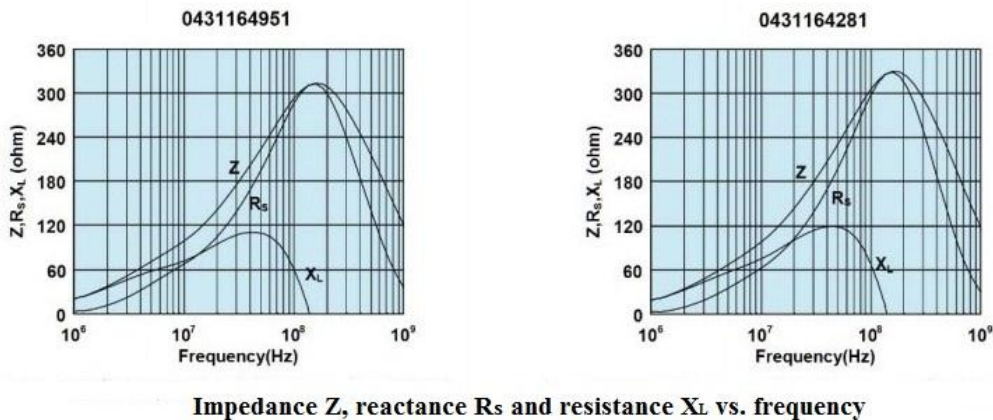
### 3.1 ECDL

Based on the existing ECDL, a few things were modified. (i) The piezo was installed onto the holder of the grating. There are two knobs controlling the grating tiltment in two directions. In order to change the length of the cavity, the PZT was installed onto the horizontal knob position. One surface of the PZT was glued onto the holder to enhance the firmness by a two parts epoxy. The cure time is about one to two hours at room temperature. To avoid the possible damage of the PZT by the hard tip of the knob, one sapphire plate (3mm\*3mm area with ~2mm thickness) was glued onto the other surface of the PZT. In order to make sure the grating only has the displacement in horizontal direction, the contact surface of the PZT should be perpendicular to the translation direction of the knob. More situations of the grating movement have been discussed in reference [13].

(ii) The laser power cables were made in order to work with the low noise driver from Vescent Technology. Each connection should be checked carefully since any erroneous connection probably causes a short circuit which possibly damages the laser diode or driver. A breakout circuit board provided by the company was used at the moment as an intermediate step between the laser driver and the laser housing. This way of connection makes the circuit-testing more convenient. The new connection diagram is shown in [Appendix B](#).

(iii) Cautions need to be paid on the isolation and shielding of the power supply cables. Because it was found that there was a 20MHz intensity modulation on the laser output, which might come from the leakage of the EOM resonance tank. Several steps are helpful to prevent the RF disturbance: (1) The power supply for the laser driver had better be independent from other electronics in case they interfere with each other electronically. (2) The cable between the laser driver and laser house better be well shielded to prevent any kind of RF source interference going to the diode driving current. (3) The cover of the D-sub connectors on the laser housing better be in metal. The cover of the connector is connected with the shielded layer of the cables, so the better grounded for the laser housing can be supplied. (4) Ferrites could be used to block the interference from RF-source under certain frequencies. Ferrite is a passive electric component and has high impedance (attenuation) in certain frequency range, see Figure 3.1. The exact turning frequency between the high and low attenuation depends on the particular configuration. One disadvantage of using the ferrite is that it might reduce the laser driving current bandwidth, but with a careful selection of the ferrite, this problem could be minimized. In this platform, two kinds of ferrite were used, both bought from Farnell (model number: 0431164951 Farnell code: 146-3432 and 0431164281 Farnell code: 146-3447). They helped to remove more than one third (this was tested when the good EOM shield haven't be done) of RF noise on the laser. Figure 3.2 shows the metal cover of D-sub connectors and ferrites used on the laser driving cables.

**Impedance Curve**



**Impedance Z, reactance R<sub>s</sub> and resistance X<sub>L</sub> vs. frequency**

Figure 3.1. The impedance curve of the ferrites used in the system.

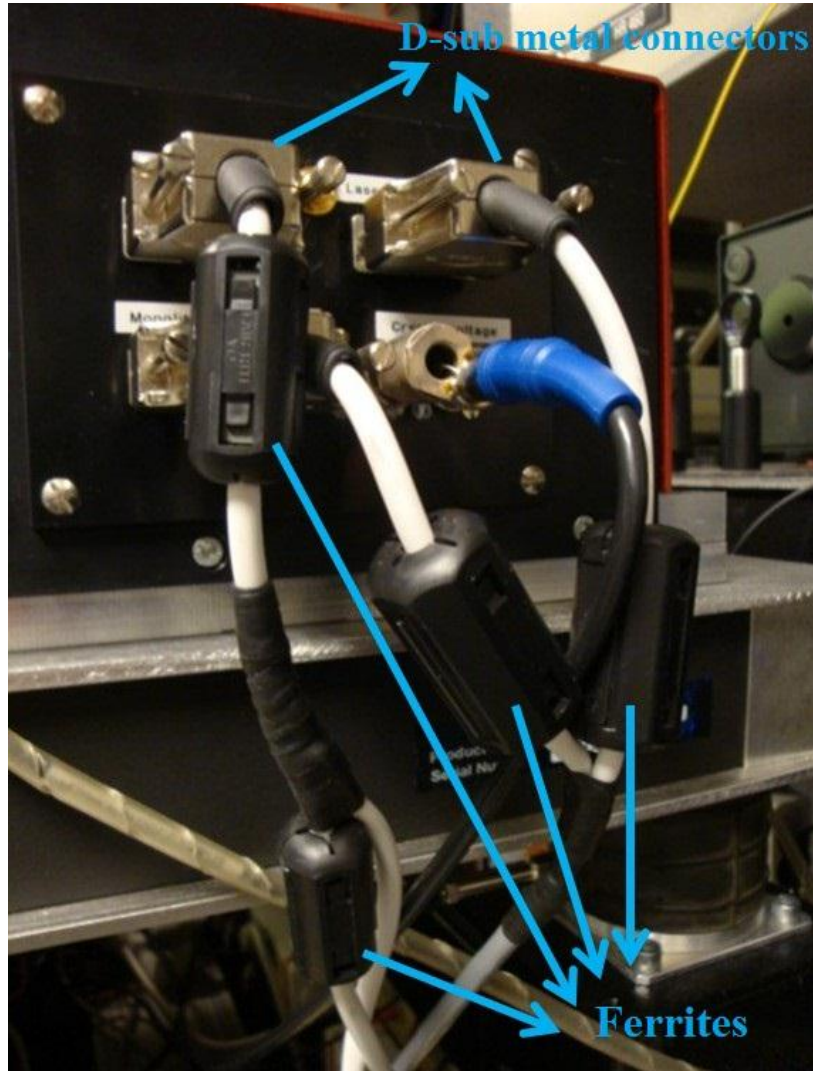


Figure 3.2. The metal pin connectors and ferrites for the laser house.

## 3.2 Ultra Low Expansion cavity spacer

This section I will introduce how we put together the ULE cavity assembly into a vacuum chamber. There are several steps involved. First, everything inside the vacuum chamber should be cleaned carefully. Ethanol is recommended as a good cleaning liquid, because there is no residual left after cleaning and no chemical reactions. If possible, clean the components in an ultrasonic cleaner [14]. Second, bake all components in the vacuum chamber to get rid of the gasses trapped in the material to large extent. This will be introduced in [Section 3.2.1](#). Third, put every component into the correct places ([Section 3.2.2](#)). Fourth, seal the vacuum chamber ([Section 3.2.3](#)).

### 3.2.1 Bake out all components

Outgassing is a problem to maintain the ultrahigh vacuum environments. It is an important issue to be considered and NASA provides a datasheet for some low outgassing materials [15]. The outgassing always comes from the impurity and material itself, so besides cleaning, the baking out process is very helpful. The lower the pressure wants to go the higher the baking temperature is needed, e.g. if the pressure want to reach below  $1.3 * 10^{-8}$  mbar, the vacuum baking system probably need to be heated around 200 °C with the pumping system running [16]. Here the target pressure is around  $10^{-8}$  mbar, so a high baking temperature above 200 °C is needed. But there are some components cannot stand very high temperature, in that case extending the baking time is helpful. Table 2 summarizes the maximum baking temperature of each component, which will be used in the vacuum chamber. The limiting component is the plastic handwheel of the valve, which is used for controlling the entrance to a turbo pump. However it can be unplugged.

Table 2. The maximum baking temperatures of the components

Components	Baking temperature	Components	Baking temperature	Components	Baking temperature
Gauge of Turbo Pump	150 °C	PEEK shrink tube from Accu-Glass	250 °C	Plug atmosphere side	180 °C
Conductance wire with Kapton insulation	250 °C	Epoxy for UHV Accu-Glass	Operating temperature to 250 °C	Plug vacuum side	140 °C
Steel	450 °C	Viton rod	150-200 °C, depending on type	Electric feed through on a CF flange	350 °C
viewport	200 °C 3 °C/minutes	Crimp contact Gold plated	200 °C	Valve body	150 °C
Copper gasket	450 °C	TECs	200 °C	Hand wheel	120 °C
PTFE shrink tube	260 °C	Temperature sensor	300 °C		

The baking out process followed the Steps 1-6.

Step1. Put all components need to be baked into the vacuum chamber, and seal the vacuum chamber properly.

Step2. Covered the glass view port with some aluminum foil as shown in Figure 3.3. To avoid the direct contact between the heating band and the view ports. The point is to use the thermal radiation rather than convection. In that way the increasing of temperature of the view port is more evenly.

Step3. Wrapped the heating band around the vacuum chamber as uniform as possible, trying to avoid the heating band folding upon itself. Because the overlapping heating band could give rise to a higher local temperature which possibly damages some sensitive components.

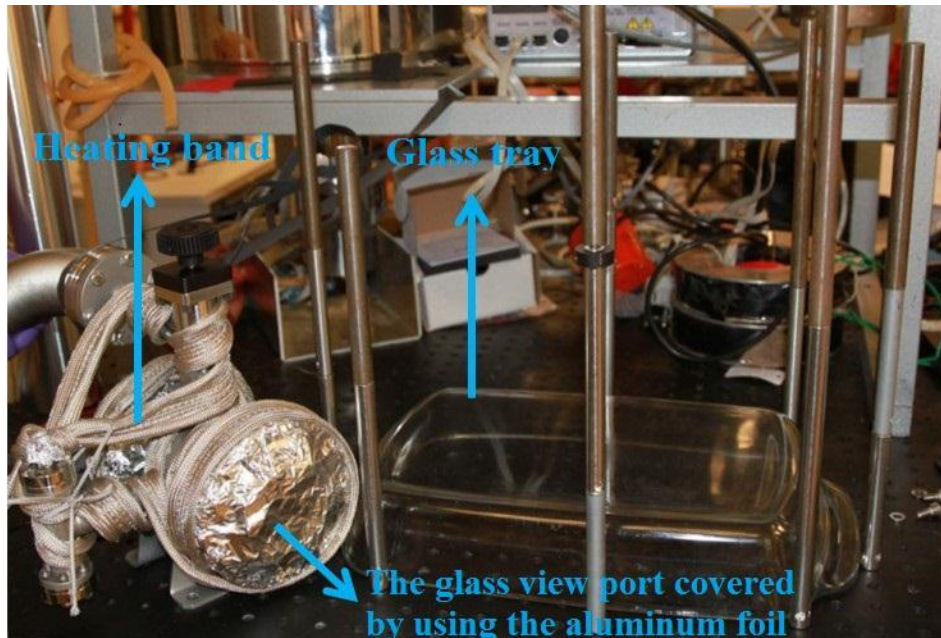


Figure 3.3. The baking out step 1-3.

Step4. Wrapped aluminum foils around the heating band to reflect the outgoing thermal radiation back to the vacuum chamber. Four independent temperature sensors were inserted to monitor the temperature at two view ports, main body of the chamber and the valve body (setting here because the baking temperature for handle wheel is a limitation). Figure 3.4 shows the temperature probes position.

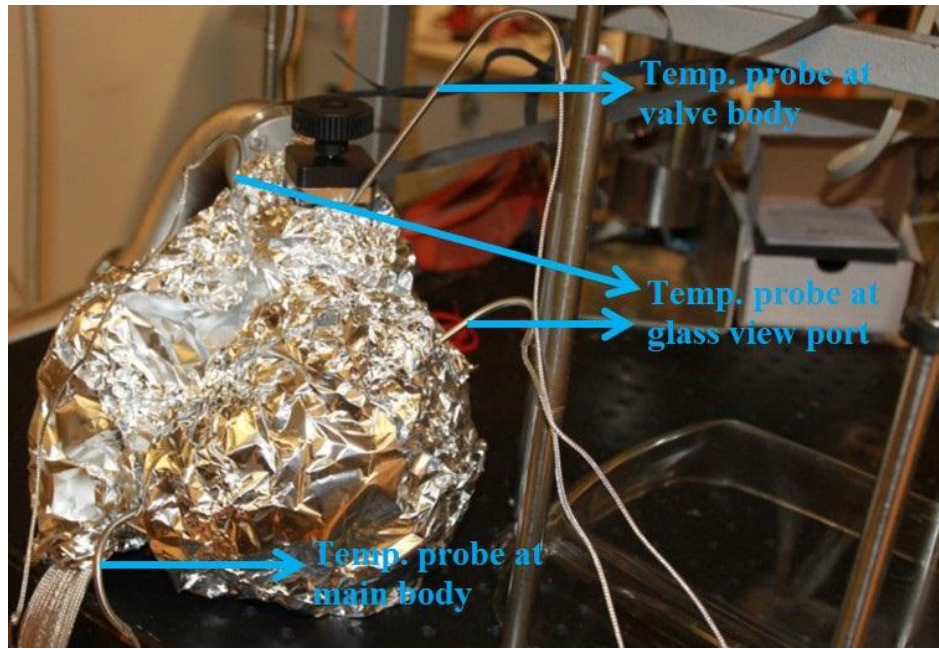


Figure 3.4. The baking out step 4.

Step5. A blanket was used to cover the whole vacuum chamber assembly, to prevent the heat dissipation into the environment and increase the heating speed. Meanwhile, to avoid the high baking temperature influence other devices on the optical table, one glass tray was placed upside-down on the table. And the vacuum chamber assembly sits on top of it. Several posts were fixed around the chamber as safe guards in case the assembly is falling off accidentally. Figure 3.5 shows the final state of the baking out. Up to now the baking out preparation work was done.

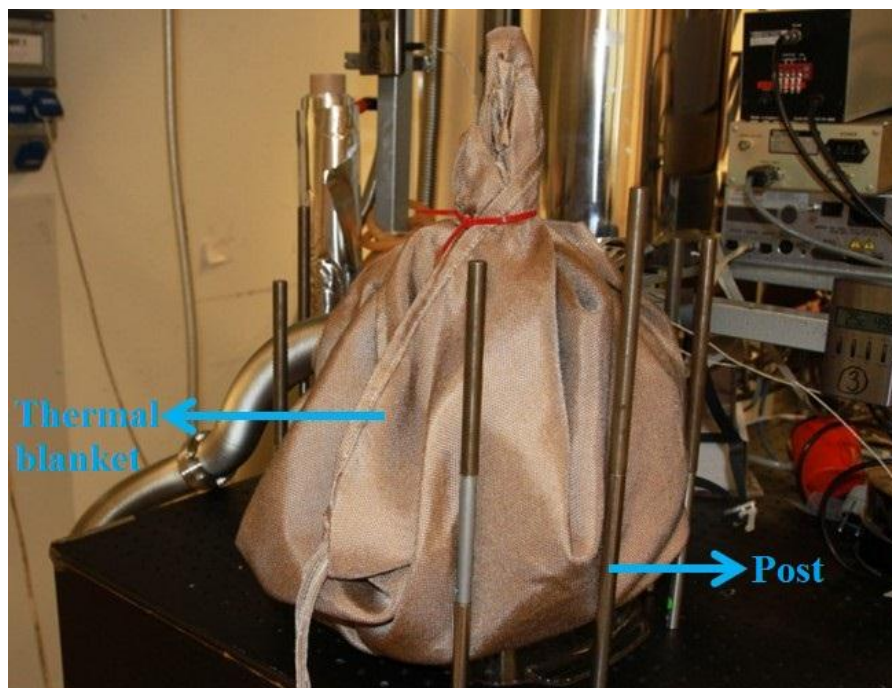


Figure 3.5. The baking out step 5.

Step6. Turn on the heater and increase the supplying voltage gradually. From the temperature monitor, one can read the instant temperature for different parts, and control the heater in a reasonable speed. In one minute the temperature change should be lower than 3 °C, because the windows might crack due to too quick expansion or contraction.

Figure 3.6 shows the temperature and pressure of the first time baking out. For this vacuum chamber the pressure is going down very quickly from  $4.6 \times 10^{-6}$  mbar to  $4.6 \times 10^{-7}$  mbar after two days baking with a maximum temperature of 80 °C. When the baking temperature was increased, the pressure went up due to the outgassing. After several heating and cooling cycles, the temperature variation does not influent the pressure as prominent as before. Finally after 10 days, the pressure arrived to  $4.0 \times 10^{-7}$  mbar by using the turbo pump.

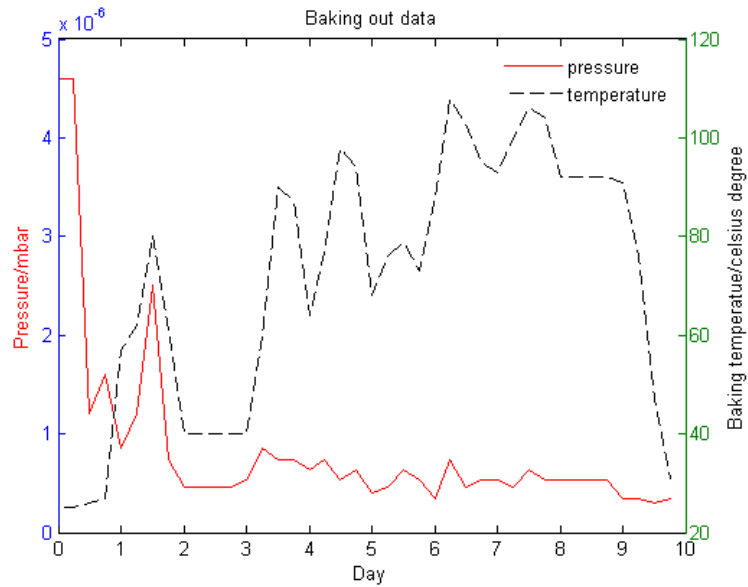


Figure 3.6. The first baking out data

[Appendix C](#) shows more records of the baking out just as a reference for someone who want to do similar works.

### 3.2.2 The ULE cavity assembly

After the baking out, the ULE cavity was installed into the vacuum chamber. **First step**, four copper adapters were glued onto the inner wall of the vacuum chamber, shown in Figure 3.7. These four adaptors will support the radiation shield. Before glue the adapter, the proper position should be found. One can put the radiation shied into the chamber and look for the correct adapter position, and then glue the adapter one by one. The vacuum compatible two parts epoxy glue was used. The glue is not conducting the heat very well, so the thickness of the glue layer should be as thinner as possible. The cure time of the glue is around 8 hours at room temperature, so heating the chamber body is a good choice to save time. To avoid the

adapters change their positions, four clamps were used to fix the adapters until the glue was cured.

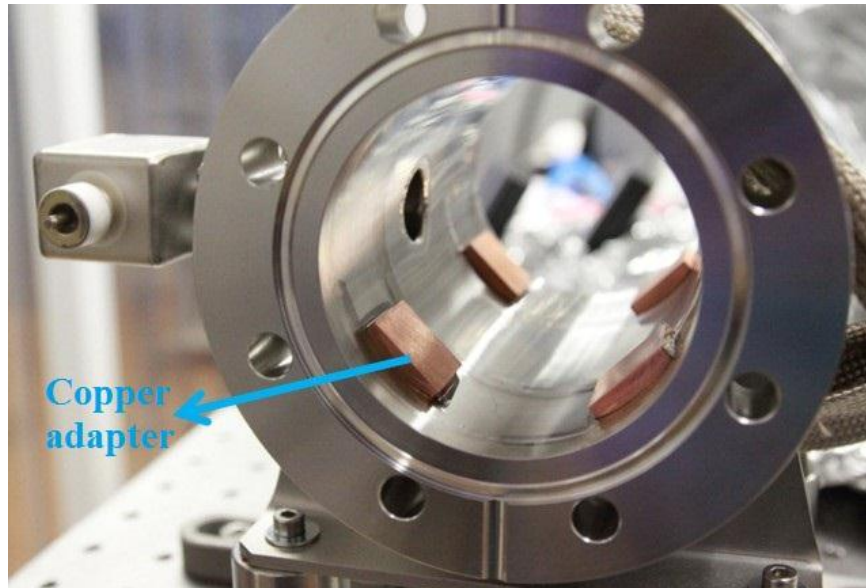


Figure 3.7. Four copper adapters were installed

**Second step** is similar to the previous step, where the TECs were glued onto the adapters. Here several things should be noticed: (1) The TECs wire connection should be designed and connected well making sure the cables are not on the way then the ULE spacer is installed later because there is only 3mm gap between the ULE spacer and the inner wall of the vacuum chamber. An illustration of the TECs connection is shown in Figure 3.8.

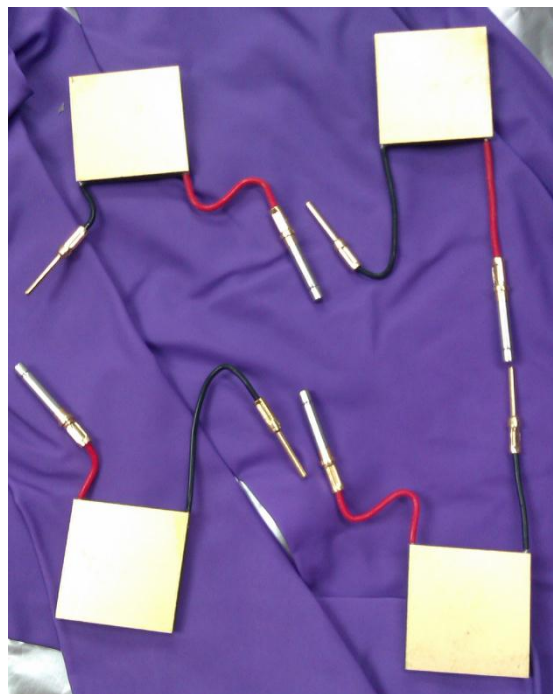


Figure 3.8. TECs connection. Four TEC were connected in series by crimp contacts.

(2) The wires and connectors on the TEC are not insulated (in Figure 3.8, the wire insulated type was ordered), so the insulation protection is very important. (3) TEC is a fragile device and any soundable collision will possibly destroy it even though it is not cracked, so in this step, one need circumspection and patience. Before and after this step, the TEC testing is necessary. Using a multimeter to test the impedance is a choice but the value varies with temperature and how well the wires are insulated, etc. It helps to identify if there is a break out in the circuit but it is not enough to tell if the TEC works as it should. Another choice is to connect it to a power supply, supply the suitable voltage to it (according to the data sheet of the TEC) meanwhile monitor the current value to see if the current is as it is expected from the datasheet. Again heat the chamber to speed up the glue cure time. Figure 3.9 shows the chamber after the TECs were installed.

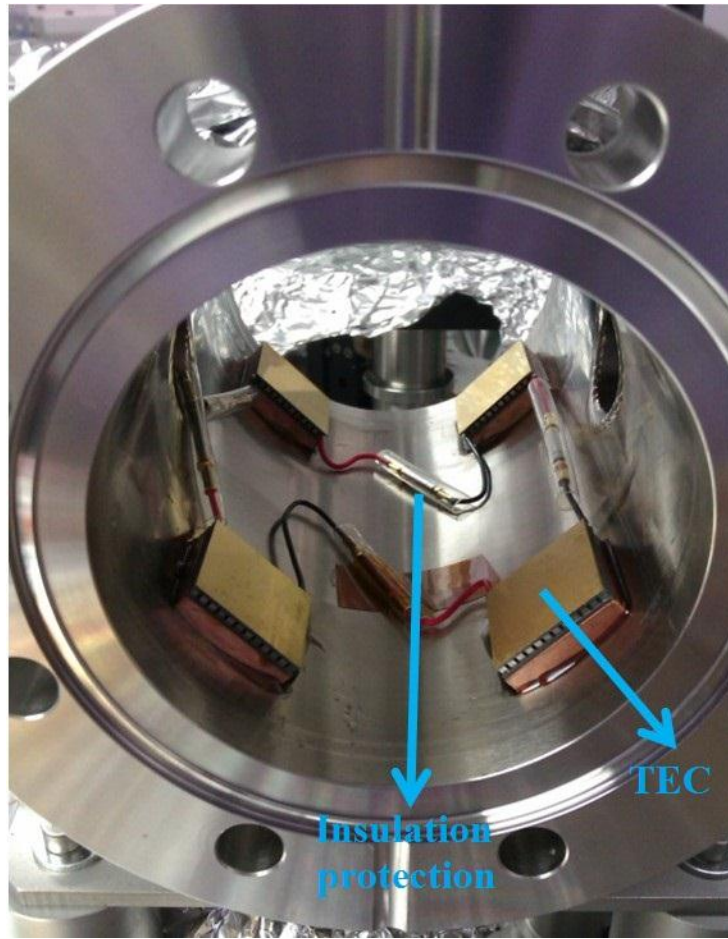


Figure 3.9. The TECs were installed

The **third step** is assembling the ULE spacer into the radiation shield. Four sets of screws, spring wires and Viton rods were used for holding the cavity onto the radiation shield. Figure 3.10 shows the structure when the installation was done. When the thin spring wires hold the spacer, in order to predict the deflection, a rough beam calculation was done by Yan. The spring wire with 0.5mm diameter was used. Its length is 11mm. The assembling process followed the following procedure. (1) Slide the ULE spacer into the radiation shield. Rotate the radiation shield gently until the sink holes are in vertical direction. (2) Insert some gaskets

(here the cleaned Viton rod and aluminum foil were used) under the ULE spacer to push ULE spacer up closer to radiation shield. (3) Put the four Viton rods into the sink holes. In the middle of the Viton rod there is a small hole (diameter is 0.52mm) for connecting with the spring wire, so the surface of the Viton rod should face the hole. (4) One person used a flashlight illuminating the Viton rod, another person inserted the spring wire into the Viton rod by using a tweezer. (5) Screw the socket button head screws into the radiation shield and let the spring wire go into the small hole (diameter is 0.52mm) in the center of the screw.

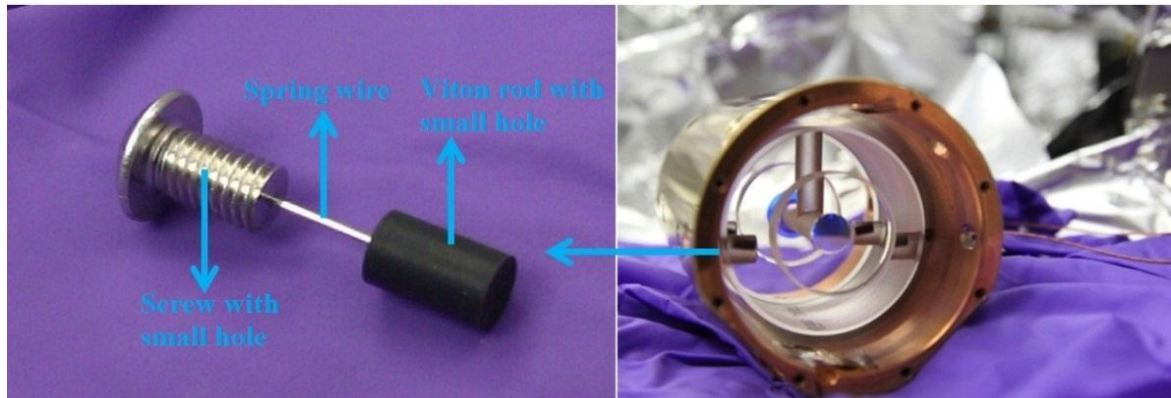


Figure 3.10. The structure of the ULE spacer hanging onto the radiation shield.

The **fourth step** becomes easier, putting the radiation shield into the chamber. During this process, the wires of the sensor might be blocked by the TEC, so this step needs patience as well. One person pulls the wires out from the feed through port gently and another person pushes the spacer into the chamber gently. In order to fix the radiation shield, the epoxy glue was used again. Some Viton rods were used in-between the radiation shield and vacuum chamber to hold the radiation shield position until the glue was cured. Figure 3.11 shows the situation.

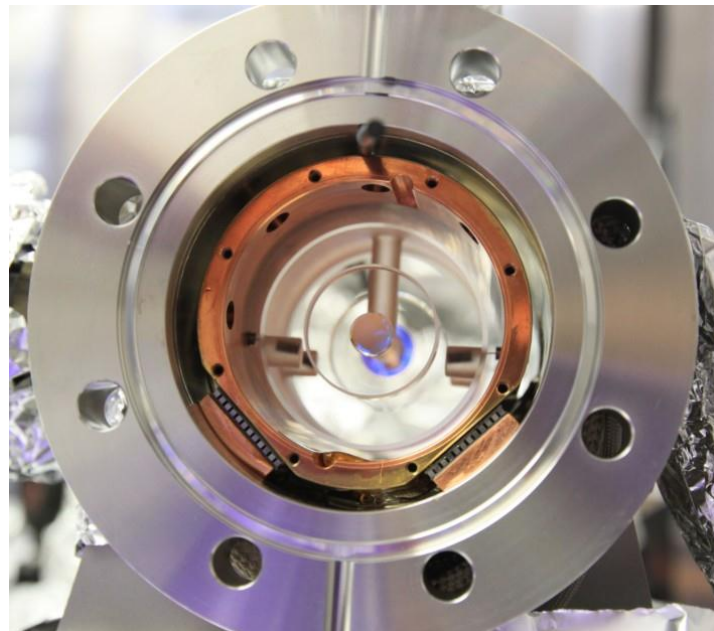


Figure 3.11. Putting the radiation shield into the vacuum chamber.

Before the vacuum chamber was sealed, the circuit connection need to be rechecked. As mentioned before, there is a feed through port which connects the wires from the TECs and temperature sensor with the temperature controller outside. The feed through is shown in Figure 3.12. The left part is the outside connector, and the right one shows one plastic connector inside the vacuum chamber which is ordered from Vacom. The inside plastic connector have two types. One is the crimp contact type which should be used with the crimp tools, but we don't have the proper tools for doing that and the thin wire is very easy to break after a few times bending. So another solder type connector was ordered and used finally. Better to check all the electronic connections are working before and after sealing the vacuum chamber.

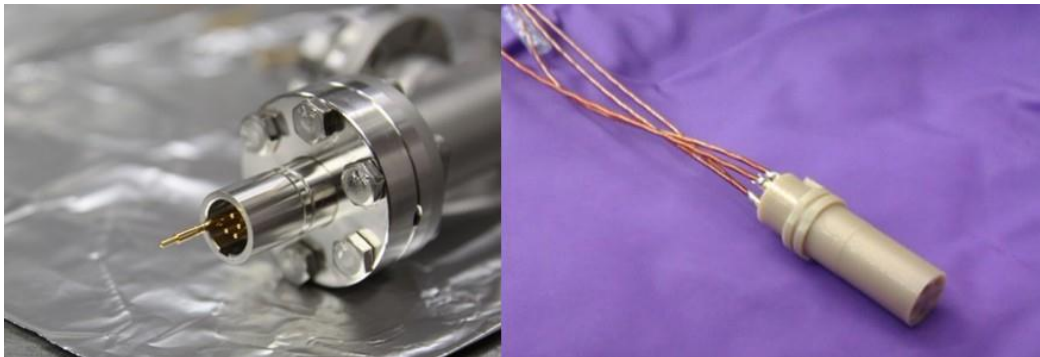
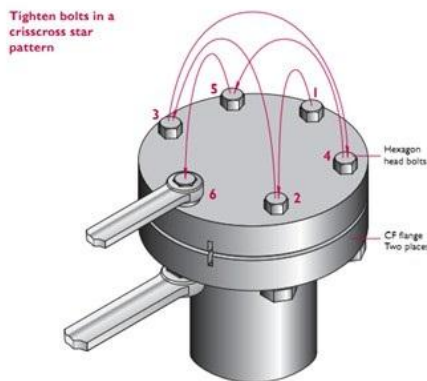


Figure 3.12. The feed through structure

### 3.2.3 Pump the chamber to vacuum

From baking out until the final assembly, the vacuum chamber was assembled and disassembled several times for different reasons, for instance baking at difficult temperature, the pressure is not low enough so that suspecting a leakage. The correct sealing method can protect the fringe of the connection flange, thereby ensure a good contact and a closed environment. Figure 3.13 shows the tighten methods and torque values used for different bolt size screws [17]. In order to protect the flange surface, the tighten blots should be in a crisscross star pattern. Better to use a torque wrench to have a good control.



Bolt size	Torque
M4	9 Nm
M6	16 Nm
M8	20 Nm
<b>Vacuum range</b>	
CF or wire seal	$1 * 10^{-13}$ mbar
Elastomer seal	$1 * 10^{-8}$ mbar

Figure 3.13. The tighten method and torque value used for different bolt sizes [17].

The vacuum chamber has been mentioned in [Section 2.3.2](#). There are two steps for pumping the chamber to high vacuum. First, starting with the turbo pump the pressure can go from atmospheric pressure down to  $4.0 * 10^{-7}$  mbar. For an even lower pressure, the ion pump should be used. The next step is to turn on the ion pump. The datasheet of the ion pump states, one needs to close the valve to turbo pump completely before starting the ion pump. However that did not work because the ion pump was automatically shut down giving an error message complaining that the pressure is too high. The reason might be that if the pressure is too low when starting the ion pump, the controller might be supplying too much power than estimated for the given pump size and in that case it will shut down [18]. Then we tried not closing the valve completely, rather leave it about a quarter turn open, the ion pump can start working properly. Afterwards completely closed the valve to turbo pump and disconnect the turbo pump from the chamber. This situation may be an individual case on this vacuum chamber. The lowest pressure of this vacuum chamber achieved with this ion pump is  $1 * 10^{-8}$  mbar (In the end of last year, it was this pressure) after a few months pumping.

### 3.3 PDH locking setup

When the pressure and temperature of the vacuum chamber was stabilized, the laser light should be coupled into the cavity and then detect the error signal. In this section I will introduce three important optical elements (DP AOM, polarization maintaining fiber and EOM) before the beam is ready to be coupled into the cavity, and two electronic filters before the error signal detector. Figure 3.14 is an overview of the electronic layout of the stabilization system, where many components will be mentioned in following sections.

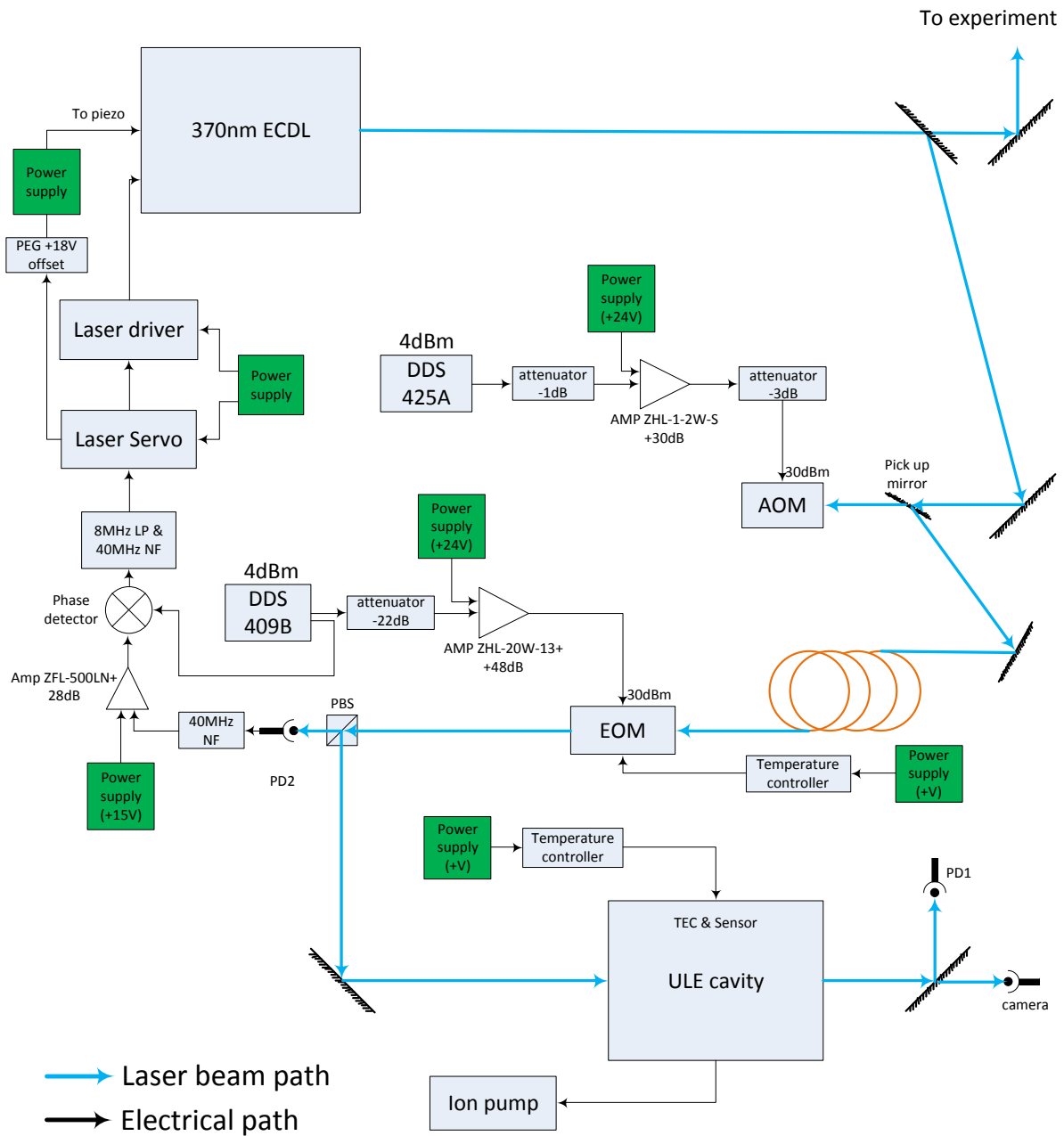


Figure 3.14. Overview of the electronic system

### 3.3.1 Double Pass AOM

DP AOM setup is mostly used for the single ion detection experiment providing 200 MHz frequency scanning ability. When one wants to search a single ion (homogeneous line width is ~3 MHz), the laser frequency need to scan at least tens of megahertz meanwhile keep the laser locked to the cavity during the scanning process. AOM consists of an acousto-optic medium and a piezoelectric transducer. When a RF signal applies to the piezoelectric transducer, it will create an ultrasonic wave to the acousto-optic medium, and the reflection index of the acousto-optic medium will be changed periodically. This refractive index change makes the medium acting like a Bragg grating to deflect the incoming laser into different orders. So the output laser frequency can be changed by changing the frequency of the RF source. But the angle of the deflected light will change as well when the RF frequency changes. This change of the deflection angle can be compensated if the laser beam passes through the same AOM twice as shown in Figure 3.15.

The RF bandwidth of the AOM is  $\pm 50$  MHz around the center frequency of 260 MHz. The active aperture inside the AOM is quite small, around 450 um. If one wants to get the first order diffraction efficiency around 80%, the diameter of the laser beam should be around 75 um. In order to get the suitable diameter of the beam, one combination of lenses were set down before the DP AOM.

The DP AOM alignment procedure is as following. For simplicity considering the incoming beam as a collimated light and the beam height is 75.4 mm (this height is determined by the laser source). The AOM should be set at the focal point of L1 (in Figure 3.15), meanwhile the distance between AOM and L2 should be  $f/2$  (focal length of L2). Then the deflected light after the AOM will be collimated by L2. The L2 position should be checked by measuring the distance between 0 and 1<sup>st</sup> order light at near and far filed after L2, if the L2 is at the correct position the distance between those two beams should be constant all the way. The intersection angle between M1 and M2 mirrors is almost 90 degree to pick up the 2<sup>nd</sup> pass beam easily. The first incoming light was aligned higher than each other which make sure the reflected light is parallel with the incoming light. In order to prevent the overlapping between the incoming and reflected light, the incoming light should be higher than the optical axis of the L1 by about 5mm. Depending on the ultrasonic wave direction the beam will be divided into several order after the AOM.

Figure 3.15 shows the beam path. After the first path, all others orders light were blocked and only the 1<sup>st</sup> order beam propagates freely. The 1<sup>st</sup> order reflected light passes through the AOM a second time, its 1<sup>st</sup> order light is right below the incoming light. The 2<sup>nd</sup> pass beam and incoming light are vertically symmetrical around the optical center of the L1. Final the pickup mirror which is under the incoming beam will reflect the light forward.

The AOM transmission efficiency and the light movement should be measured. Firstly measure the power of the incoming light. Secondly the first order diffracted light power (at the center RF frequency) is measured around 80% of the incoming beam. Thirdly the 1<sup>st</sup> order

diffraction of the second pass was measured. The diffraction efficiency of the double pass light is around 60% at the center RF frequency and 30% at the two ends of bandwidth. To check how well the DP AOM was aligned, the beam after double passing through the AOM was coupled into a single mode fiber. If the beam position does not move within  $\pm 50$  MHz range across the center RF frequency, the fiber coupling efficiency should be almost the same. Otherwise, the up and down mirror should be fine adjusted. If this doesn't help the AOM position could be fine adjusted as well.

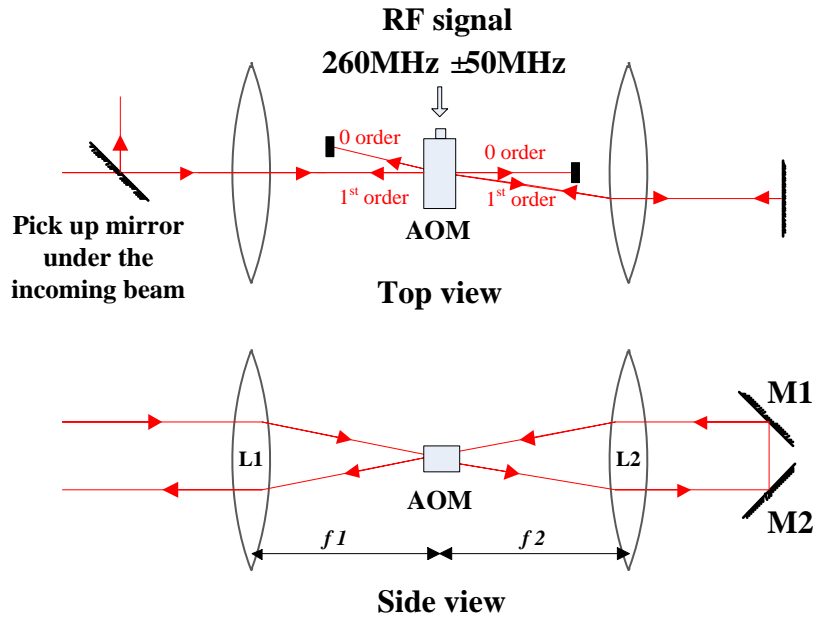


Figure 3.15. Double pass AOM setup

### 3.3.2 Single mode polarization maintaining fiber

After the beam passes through the AOM, there is big risk that the spatial beam profile has been distorted. To get one well shaped spatial mode the light is coupled into a single mode polarization maintaining (PM) fiber before the beam is coupled to the cavity. The single mode fiber only supports the fundamental mode ( $TEM_{00}$ ) and all other modes will be heavily attenuated and thereby filtered out. The fiber (referred as stabilization fiber) is 50 cm long and was bought from Thorlabs (model PM-S350-HP). Coupling the laser beam into a signal mode fiber is a very tricky task, especially when the spatial mode of the laser itself is not good. Figure 3.16 shows the beam path of the fiber coupling. At the beginning, trying to use the reflected light from the fiber as a guidance and then adjust the two mirrors in front of the fiber to overlap the incoming beam with the reflected light. But because of a few reasons, it is very difficult to achieve a coupling efficiency of more than 1%. Those reasons are: (i) It is not easy to get a well-defined reflected beam from the fiber. Most often the reflected beam looks like cutting somewhere because the beam is not sufficient close to the correct path. (ii) Mirror 1 used for adjusting the input beam tiltment is a little far away from the fiber, because there are

more optics in between of them. Thus it makes the beam movement at the fiber position is so sensitive to the adjustment of that mirror. (iii) The spatial mode of the output from the laser diode is not good. That provides local maxima when coupling into a fiber. In this situation, another way was applied. There is another piece of fiber (referred as experimental fiber) on the platform. The laser is already coupled into it. So we disconnect the experimental fiber from its own output coupler and connect it onto the input coupler of the fiber which we want to couple light into. Then use the output laser from the experimental fiber as a guiding light for the beam alignment. Later the fiber transmission efficiency was tested. Here, several times testing were done. The light is after the DP AOM, when the RF signal for AOM at the center frequency, the transmission efficiency is around 40% and at the ends of the bandwidth, the transmission efficiency is around 35%. The testing result is a good criterion to judge the DP AOM alignment, and the testing result proves this alignment which fulfills the requirement.

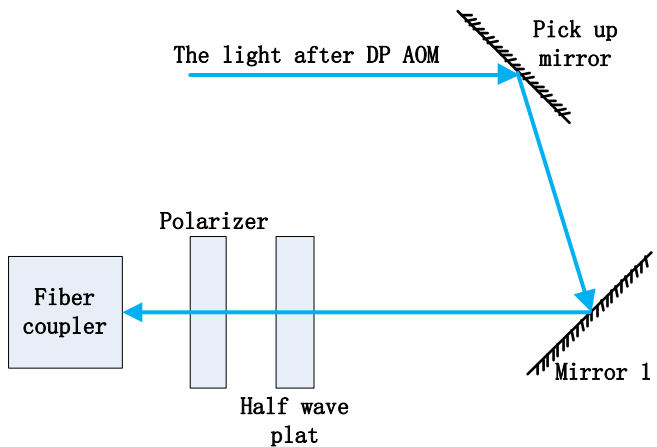


Figure 3.16. The beam path of the fiber coupling

After the laser is coupled into the fiber, the polarization state of the laser should be measured and adjusted. Here, one halfwave plate and polarizer was set up before the fiber to adjust and purify the laser beam polarization state. Our stabilization fiber is a panda type fiber. For this type of fiber there are two axes, one is called fast axis (the direction having a low refractive index) and another one is slow axis (with a high index of refraction). Typically when the light polarization is along the slow axis, a better polarization maintaining is achieved [19] and the direction of the slow axis is often indicated on the fiber connector by the manufacturer. How well the polarization maintaining of the fiber is can be tested by slightly changing the temperature of the fiber and watch the throughput power of a polarizer which sits after the fiber output collimator. If the input beam polarization is not exactly along the fiber slow axis, the throughput power will change obviously when holding the fiber by hand. Another way is to measure the extinction ratio [19] at the fiber output, when the extinction ratio get the largest value which means the polarization state has the best match between the laser beam and the fiber. Comparing the angle position of the polarizer in two testing methods, the discrepancy is around 2 degrees.

### 3.3.3 Electro Optic Modulator

The electro-optical crystal inside the EOM is a birefringent crystal. When the incoming laser beam has a polarization state not matched with one of the crystal axis, the polarization state of output beam will be turned, which could cause the residual amplitude modulation (RAM) on the laser beam [20]. The modulation frequency is exactly the EOM input RF signal frequency. The RAM signal could be wrongly taken as the error signal since they have the same frequency. To avoid the RAM, one needs to find the EOM crystal axis and align the input beam polarization along one of the axis. Measuring the extinction ratio is a convenient method. Use two cross polarizers to do that. One sits before and one after the EOM. If the incident beam polarization matches one of the crystal axis, the out coming beam will not be rotated. So the throughput from the output polarizer is minimized. Otherwise there will be some throughput. Change the polarization orientation of the first polarizer and the second one correspondingly (make sure they are always perpendicular) as well until the throughput intensity is minimized. An extinction ratio of 39 dB was measured. One also needs to make sure the input beam polarization should be in vertical direction, if not slightly rotate the EOM orientation.

As mentioned in [Section 2.4.2](#) in order to get high enough voltage to achieve the reasonable modulation index, a resonance tank is used. **First of all**, one needs to check the resonance frequency of the tank. The design resonance frequency of the resonance tank is 20MHz, it means that at 20MHz the impedance of the circuit is  $50 \Omega$  so that the signal reflection is very low, but at other frequencies the reflection is a lot higher. Possibly the RF amplifier will be damaged instantly. The testing tools include a signal generator with frequency sweep and marker output function, a coupler and an oscilloscope. Figure 3.17 shows the connections between them. The output of the generator should be set in frequency sweep mode and the range covers the testing frequency (e.g. from 15 to 25MHz) and the marker signal can start with 20MHz. The coupled port of the coupler is the reflection signal from the resonance tank. Figure 3.18 shows the testing result recorded by an oscilloscope. One can change the starting frequency of the marker signal to indicate the resonance frequency. During these test, one need to make sure all equipment has an input or output impedance of  $50 \Omega$ .

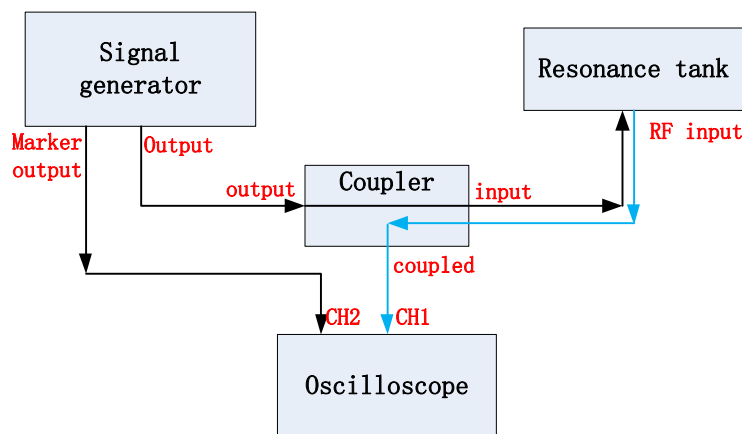


Figure 3.17. The resonance frequency testing

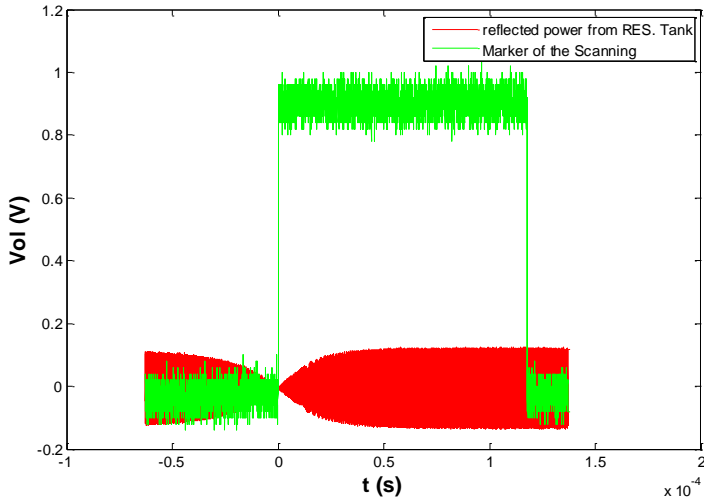


Figure 3.18. The resonance frequency testing result

**Secondly**, the modulation index should be measured. It tells how much power is distributed on the carrier and sidebands respectively. This value will influence the strength of the error signal. The modulation index can be tuned by changing the input RF power to the resonance tank. Based on the modulation index measurements done by Yan, when the input power is  $\sim 34$  dBm ( $\pm 1$  dBm) a modulation index of 1.08 was achieved which is the optimal value we want [1].

When the input RF signal power is more than 1Watt or the Lab temperature varies, the temperature of EOM will be changed and the stability for EOM will be influenced. Thus, one heating band and a temperature sensor (NJ28MA0103H from Farnell) were installed on the EOM, and then they are connected to a temperature controller (HTC-1500, Wavelength Electronics). It stabilizes the temperature of the EOM to a temperature slightly above the room temperature. Figure 3.19 shows the configuration of the EOM. The two aluminum covers not only protect the optical aperture of the EOM but also reduce the RF signal leakage from EOM. In next paragraph, the RF shielding will be continued to discuss.

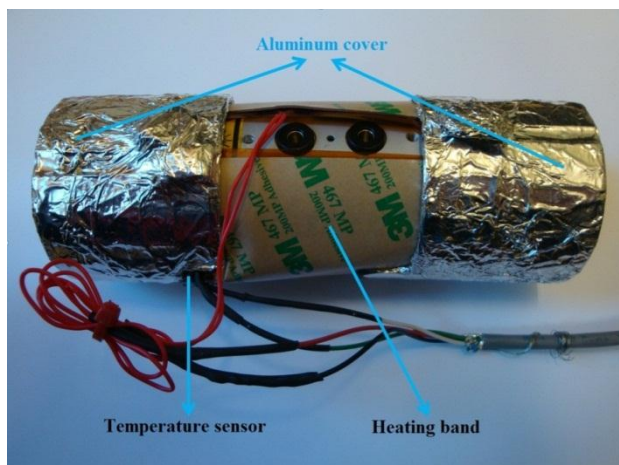


Figure 3.19. The configuration of the EOM with the heating band and aluminum cover

**Thirdly**, one should make sure there is a good contact between the resonance tank and the EOM, and the EOM should be grounded well. If the connection is not good, the EOM will become a high power RF radiator which will disturb the error signal detection and could also interfere with the laser driver to create an intensity modulation on the laser output, which once was a big trouble for us. The effective way to prevent this is to ensure a good contact between the EOM and tank, and shield the tank as good as you can. For getting a good contact, one copper adapter is made which increases the contact area between the resonance tank and EOM electrodes, as shown in Figure 3.20 Finally a better contact was achieved and the resonance tank has been grounded, thus the RF shielding is satisfactory.

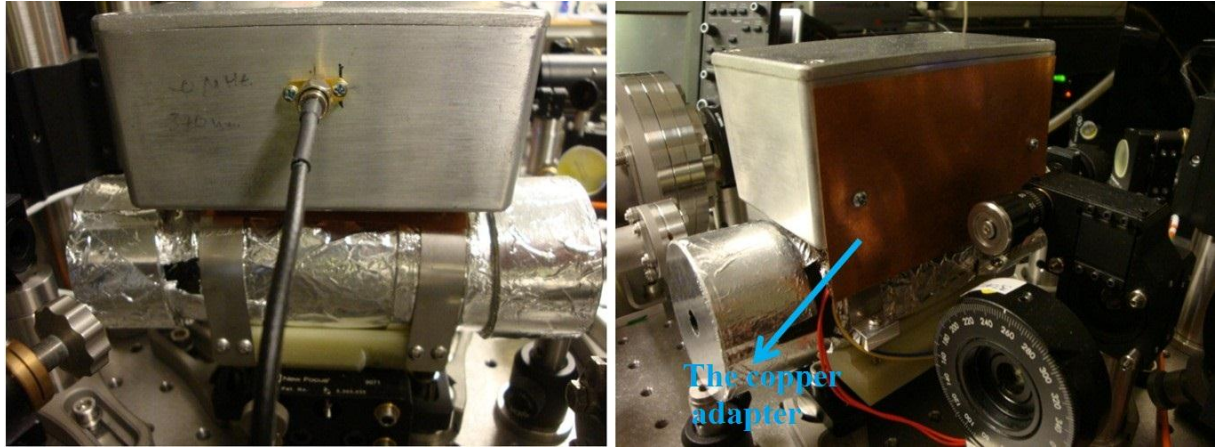


Figure 3.20. The EOM with resonance tank

### 3.3.4 Electronic Filters

Two electronic filters were used in the system, Figure 3.1 shows the connections. One is the 40 MHz notch filter which sits after the error signal detector. The function is to kill the 40 MHz frequency components in the reflected beam from the ULE cavity. The other one include an 8 MHz low pass filter and a 40 MHz notch filter, which is placed after the phase detector. The low pass filter is aiming for filtering away the high frequency components above 8 MHz (As a rule of thumb, this turning frequency should be roughly 1/3 of the phase modulation frequency) in the electronic signal carrying the error signal.

Both filters were designed in the diplexer mode which has the low signal reflection. Firstly design the circuit diagram according to the requirement. The parameter for each component in the circuit should be determined [21]. Secondly, the simulation for the circuit should be done. By using Micro-cap do the simulation and the impedance match curve can be got, the better impedance matches the lower signal reflection is. Figure 3.21 shows the simulation result. At 8MHz the signal attenuation is around 3dB and at 40MHz the attenuation reaches 75dB. The result fulfills the requirement. Figure 3.22 shows the testing results which agrees with the simulation result, meanwhile the power of the reflection signal is reasonably low comparing with the input signal.



Figure 3.21. The simulation result of the filter circuits

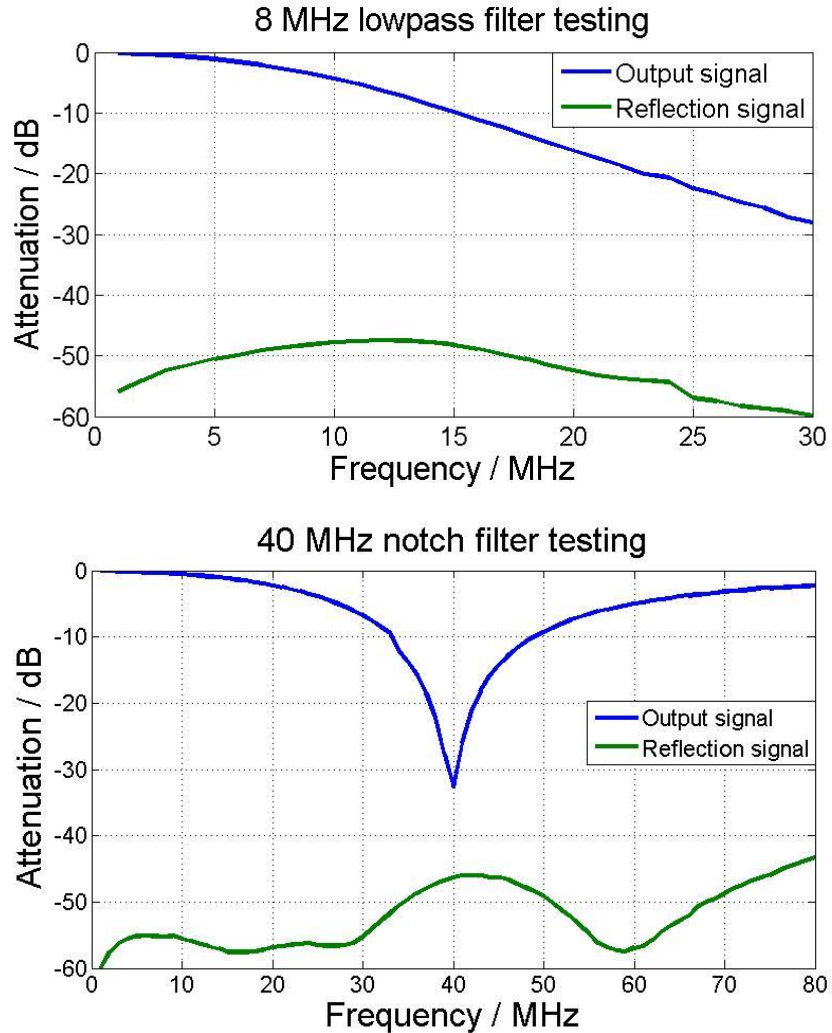


Figure 3.22. The testing result for the two filters

Thirdly, the print circuit board is designed. The design was done in Protel 99. For the circuit board, the thickness of a single layer circuit board is 1.6 mm , so the stripes should be 1.85 mm wide and the thickness is 2 um (for 50 ohm impedance) [22]. There should be a 2 mm gap in-between the stripe and the earth plane. Interconnections between the top and bottom earth plane should be made by adding some via holes. All the components' model numbers were shown under the circuit drawing and were printed on the circuit boards as well.

The circuit boards were fabricated on a custom-order from a Chinese company (SHENZHEN SEN YAN ELECTRONICS CO.,LTD). The circuit diagram and the printed circuit board are shown in [Appendix A](#).

To shield the filter, one special card-slot type aluminum boxes were ordered. This kind of box (Bopla Alubos 1040 enclosure profiles) can be sealed easily and the gaskets were selected as the electric conduction type (EMC seals DI 1040-EMV). Thus the filter has a good RF shielding. Figure 3.23 shows what the filter looks like.

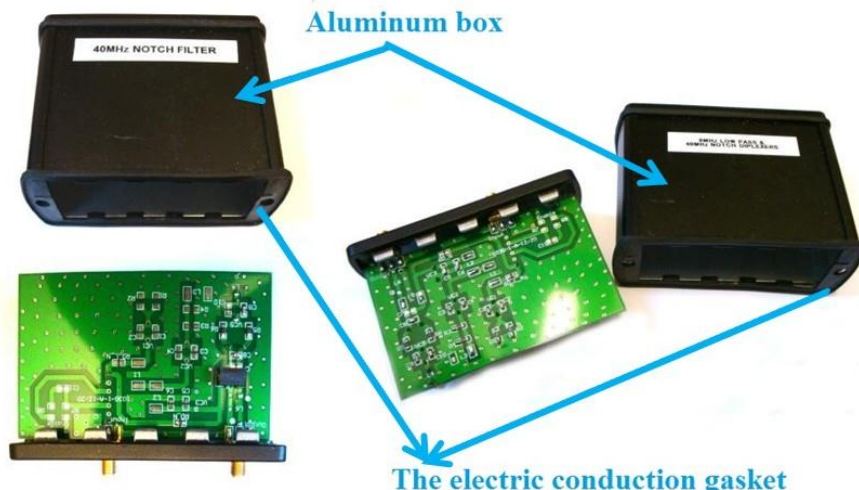


Figure 3.23. The filter boards and the aluminum boxes

Up to now, all the optical setup work is done and most of the electronic devices are set under the table. The complete platform is shown in Figure 3.24. Next work is to couple the beam into the ULE cavity to do the mode-matching, check the error signal, and feed the error signal back to the laser. These will be discussed in next chapter.

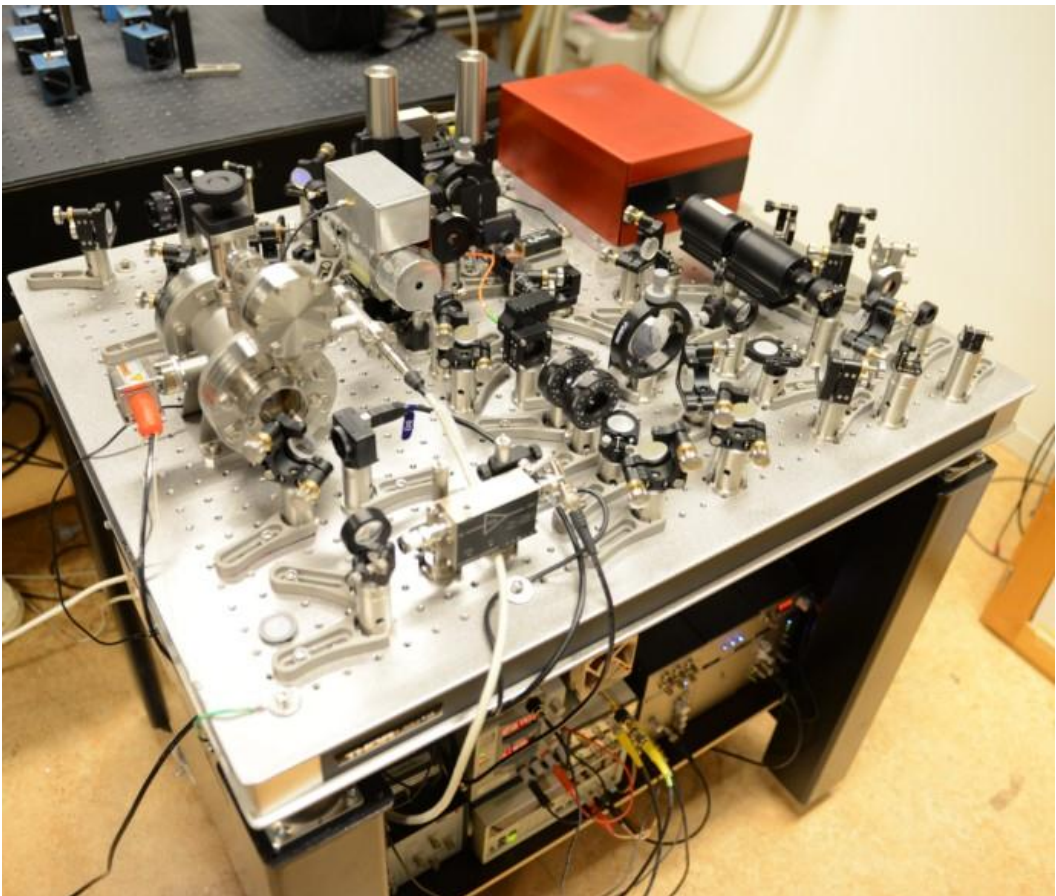


Figure 3.24. The complete platform of 370 nm laser stabilization system

## Chapter 4 Test and Measurement

### 4.1 Cavity mode matching

To efficiently do the cavity mode matching, some calculations should be done at first. The cavity mode can be determined by the length of the cavity, the separation of the longitudinal mode is the free spectral range which is equal to 2.7GHz. For this ULE cavity, the length is 55mm, and the beam diameter on plane surface can be calculated as.

$$\omega_1^2 = \frac{L\lambda}{\pi} \sqrt{\frac{g}{(1-g)}} \quad g = 1 - \frac{L}{R}$$

where  $\omega_1$  is the radius of the beam on plane surface and the result is 136um,  $\lambda$  is the wavelength of the laser,  $R$  is the radii of the concave mirror surface which is equal to 0.5.

The distance from the fiber coupler output to ULE cavity is limited by the arrangement, in order to couple light into the cavity, the incident beam has to have the same divergence as the cavity mode. One need to consider what lens is needed during the beam path, and how large the input beam diameter should be. As a guidance for the real alignment, I first ran a simulation using the ABCD matrix (initial program was written by another Diploma worker, Adam Wiman) in Matlab to check what focal length lens is needed [23], where the beam at the lens surface should have a certain input beam diameter with certain divergence. During the simulation, the refractive index for each component and the distance between each other were checked. This simulation assumes the end surface is the plane mirror and the light emit from here. Figure 4.1 shows the simulation results, where the blue lines mean the interfaces which the light passes through.

In order to find the suitable lens, the following steps were done. (i) The output of fiber collimator position is fixed, and the output beam divergence can be tuned in a small range by adjusting the position of the collimating lens surface 6 in Figure 4.1. This variation range is a good reference for the simulation, so by using the beam profile measure the variation range. (ii) Adjusting the fiber collimator divergence, selecting one suitable position for the lens (the surface 5 in Figure 4.1) before the vacuum chamber, and then change the focal length until the beam diameter in the variation range at the surface 6. (iii) With the simulation as guidance, setting down the focal lens, and by using the beam profile measure the beam diameter again after the fiber collimator and lens separately, the result should be close to the simulation. Some fine adjustments are needed.

The simulation result shows that the focal length of 400mm is suitable and the distance between the lens and the end surface of the ULE cavity is 484mm. The beam radius is 405.8um on the lens surface. Meanwhile the beam radius on the fiber collimator is 320.4um which fulfills the variation range.

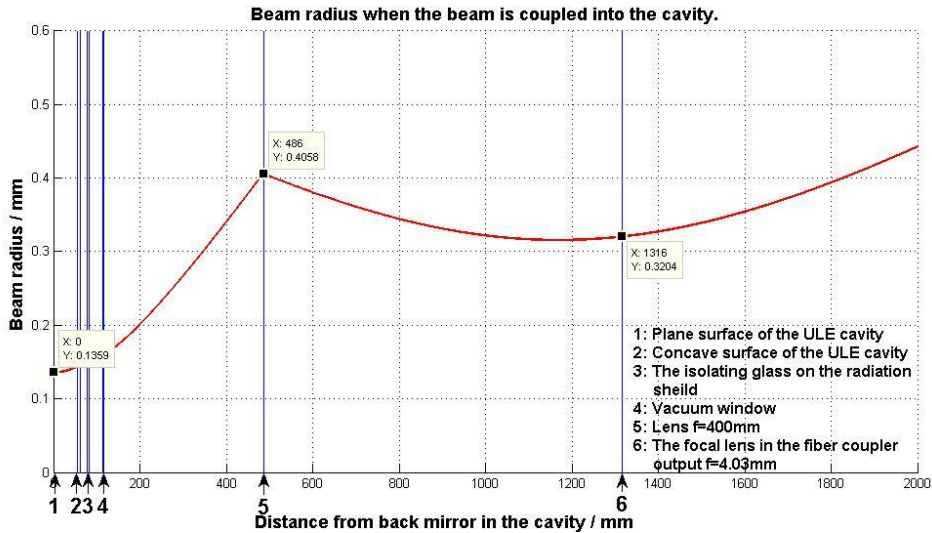


Figure 4.1. The beam sizes at different positions from fiber collimator until the ULE cavity.

After the beam diameter correction, next step is to find the correct incidence angle and position of the beam going towards the cavity to get a  $\text{TEM}_{00}$  mode matching.

First of all, one needs to put a camera after the cavity on the transmission path of the beam trying to get a signal on which to start the optimization of the beam adjustment. Then one needs to scan the laser frequency more than one FSR by scanning the PZT in the laser cavity either using an external signal generator or the RAMP function on the laser servo. The purpose is to find the resonance line of ULE cavity. Thirdly, start to adjust the beam. The light path before the cavity is shown in Figure 4.2. In order to decouple the adjustment of the beam position and its tilt angle, it is better to have one mirror rather close to the cavity, in this case is M3 and put one mirror far away from the cavity, in this case is M1. Adjusting the mirrors in both horizontal and vertical directions until one can see some patterns on the camera. Figure 4.3 shows some example transmission patterns one can see on the camera. Once you can see something, then it is just a matter of time to get a pure  $\text{TEM}_{00}$  mode.

However there are some practical difficulties, e.g. we don't have a very good control of the mode-hop-free scanning range of the laser frequency, meaning there is large possibility there are mode jumps during the scanning.

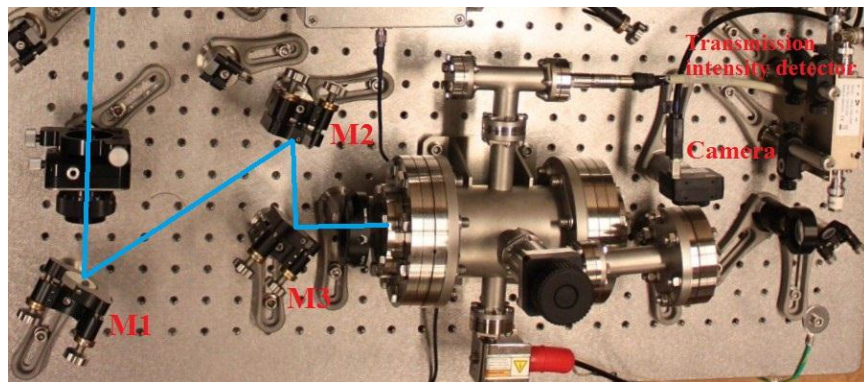


Figure 4.2. The light path before the cavity



Figure 4.3. The mode change form high order to 00 mode, left is  $\text{TEM}_{44}$  mode, middle is  $\text{TEM}_{01}$  mode, right is the  $\text{TEM}_{00}$  mode.

When the mode match is reasonably good, the transmission beam should be strong enough to be coupled into a DC detector. Figure 4.4 shows the transmitted beam intensity during one scan with the EOM phase modulation being turned off. Comparing with the input laser power, the transmission efficiency is around 2.5%, which is far away from the expected value of  $\sim 10\%$ . This might be due to the laser line width is much broader or the losses in the cavity is much larger than we thought.

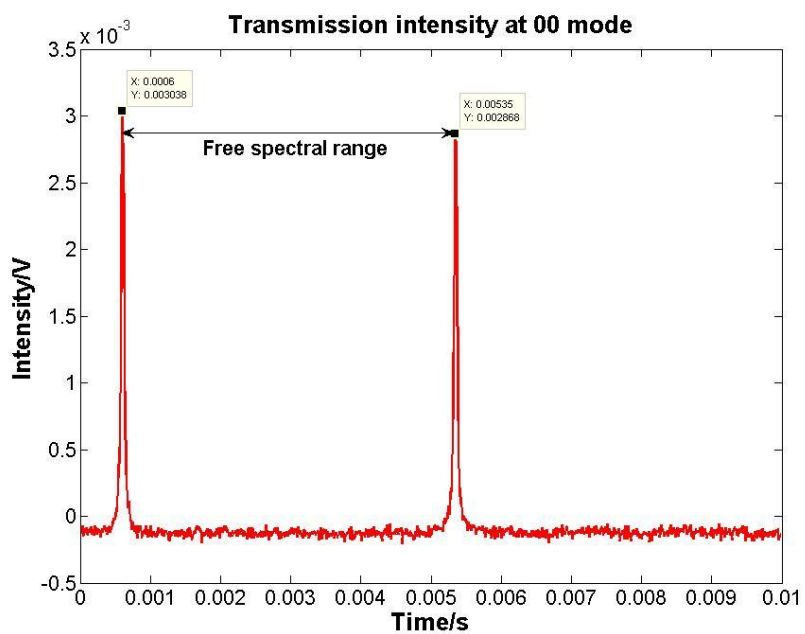


Figure 4.4. The transmission intensity curve

## 4.2 Error signal

After a good mode matching is achieved, next step is to look for the correct error signal. It should be detected with a 20MHz intensity modulation when the cavity mode is matched.

The beam carrying the error signal is the beam reflected back from the ULE cavity. The reflected beam is separated from the input beam by a PBS. The incoming beam is a pure vertical polarized light, the light polarization will be changed to right-circularly polarized after passing through the quarter wave plate as shown in Fig. 11. The polarization state of the reflected light from the ULE cavity is changed to be the left-circularly polarized. Then the polarization state will be turned by  $90^\circ$  comparing with the incoming beam. So the reflected beam is reflected by the PBS.

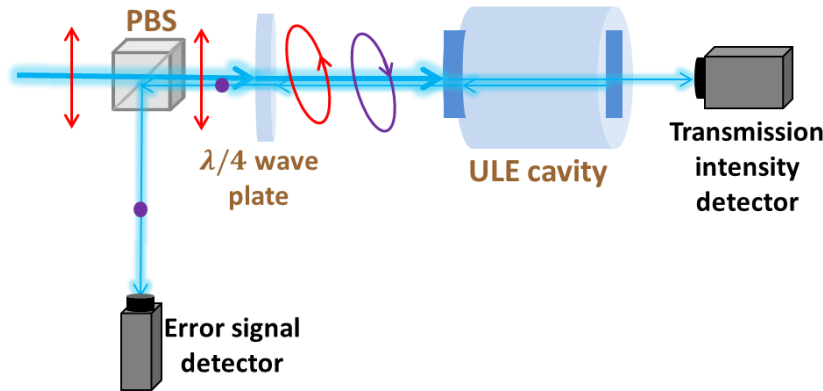


Figure 4.5. The beam path of the error signal.

The error signal is based on the phase modulation as described in [Section 2.4.2](#). First we checked the phase modulated signal on the transmitted intensity (while the laser is scanning), shown in Figure 4.6. There are two sidebands around the center frequency with a separation of 40MHz in between them. The right sideband is lower than the left sideband slightly. That is because the 60MHz (at 3dB) bandwidth limitation of the detector. The side band intensity is about 1/3 of the carrier, which corresponds to a modulation index of  $\sim 1.08$ .

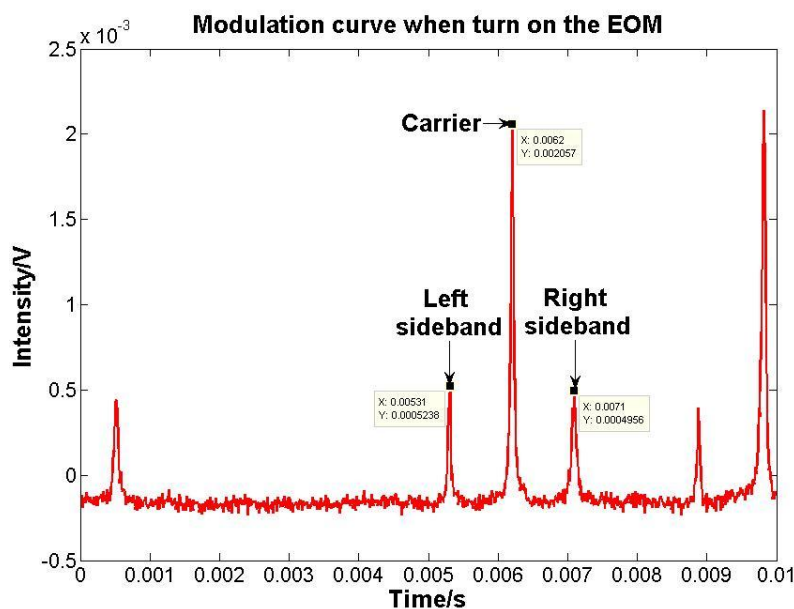


Figure 4.6. Transmitted intensity from the ULE cavity when the laser is scanning across the resonance line.

After making sure the modulation index is correct, one needs to couple the reflected beam from cavity onto the error signal detector. Firstly, one could check the monitor output of the error signal detector to see if the laser hit the detector chip. Then switch to the AC output port and record the signal. To see the 20 MHz modulation more clearly, it is better to do a FFT of the signal by using the oscilloscope which with the FFT function. Figure 4.7 shows the FFT of the reflected beam. When the cavity mode is matching very well, the strong signal at 20MHz was observed meanwhile a weak 40MHz signal also detected. When the EOM phase modulation is turned off, both signals will be gone. That means the 20 MHz and 40 MHz signal really comes from the phase modulation.

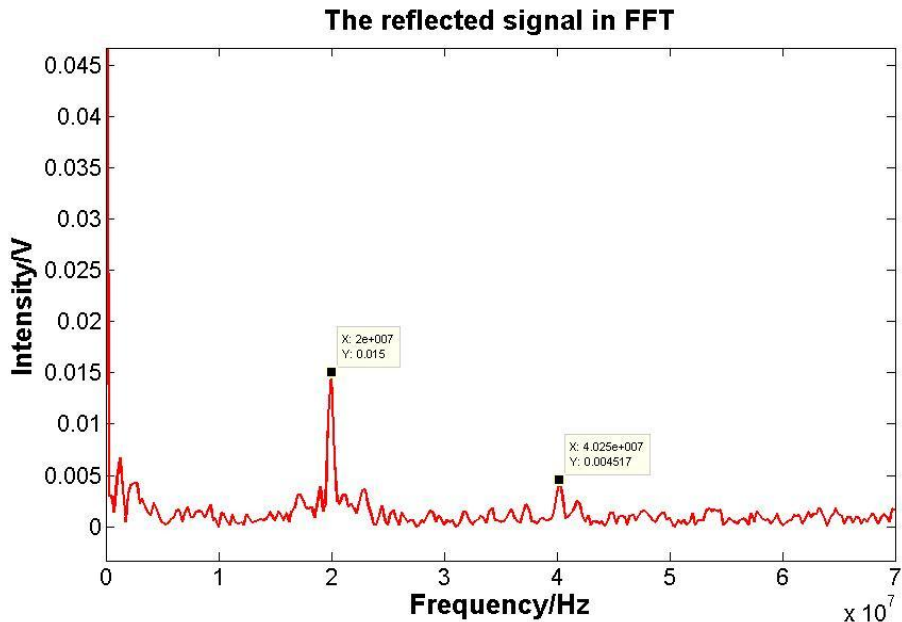


Figure 4.7. The reflected signal in FFT

Next is to feed the signal from error detector into a 40 MHz notch filter, as illustrated in Figure 4.8, the reason for doing that is to cancel the 40MHz signal which remains in the signal, here only the 20MHz signal is what we want.

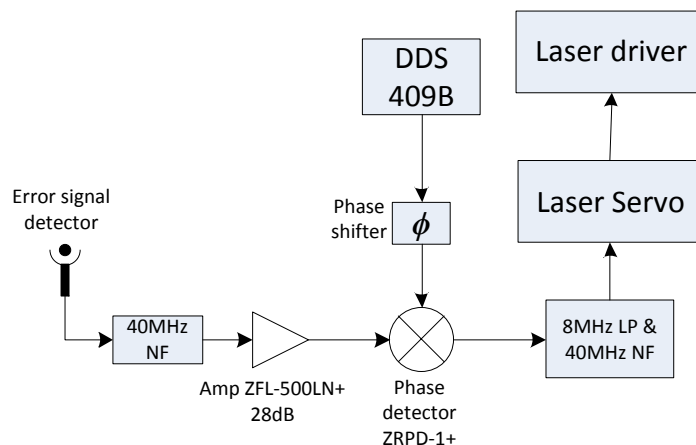


Figure 4.8. The error signal detection

Then the output is connected to a phase detector (mixer ZRPD-1+, Mini-Circuits), which multiplies two input signals and then gets the dispersion signal. In order to get the correct dispersion signal, the intensity of the two input signals should be at the same level. Here, the other synchronized signal is sent to phase detector from DDS 409B which supplies the modulation signal to EOM also. The error signal is too weak compare with the synchronized signal from DDS 409B, thus a low noise amplifier (ZFL-500LN+, Mini-Circuits) was set before the phase detector. The frequency of the synchronized signal and reflected beam signal are the same, and the multiplication result is the error signal. In order to get correct error signal, firstly make these two signals orthogonal to each other by changing the phase of synchronized signal, then the multiplication signal is 0. Let's take this phase as a reference, referring it as  $\phi$  orthogonal. Then changing the phase of synchronized signal by  $90^\circ$ , the strongest intensity can be got. Figure 4.9 shows the dispersion curve in several phase differences. The slope of the dispersion curve depends on the sweep frequency signal which is the black line in Figure 4.9. The sign of the slope should be checked when re-lock the system, next section will give more explanation about this.

The output of the phase detector goes to an 8MHz low pass filter and a 40MHz notch filter again. This filter attenuates the noise signal higher than 8MHz heavily because the error signal is a DC signal at this stage. The 40MHz notch filter has the same function as the one before the phase detector. Then we get the dispersion curve.

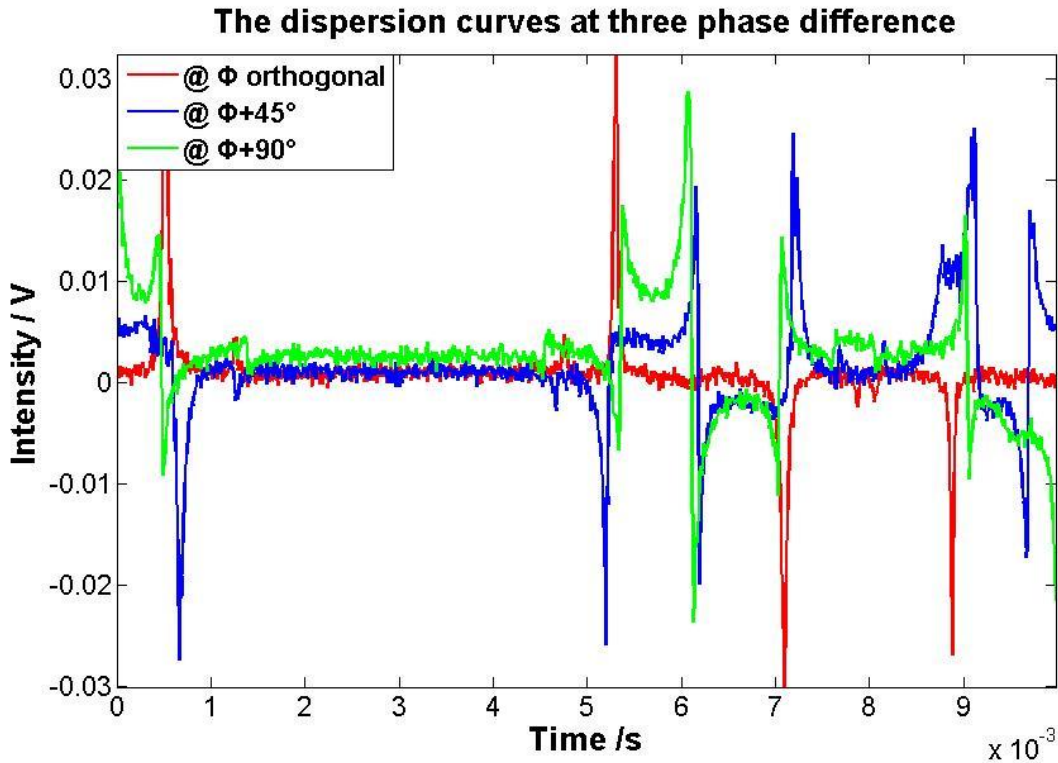


Figure 4.9. The dispersion curve at three different phase reference (negative slope).

### 4.3 Feed the error signal back to the laser servo

The final step is feeding the error signal back to the laser servo. The stabilization system can be locked in two ways. The first one is changing the laser driver current in a fast time scale ( $\sim\mu\text{s}$ ) and another one is by using the voltage to control the PZT movement in a slow time scale ( $\sim\text{ms}$ ). If the best stabilization wants to get, these two methods will be cooperated, but at the beginning one can adjust one by one. The schematic connection diagram is shown in Figure 4.10.

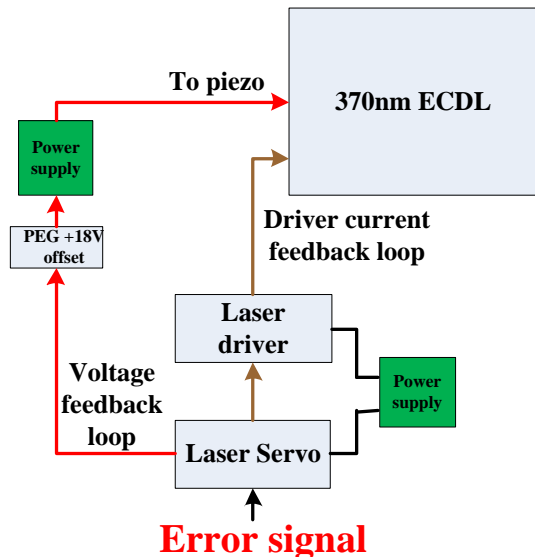


Figure 4.10. The connection diagram of the two feedback loop.

Firstly, the current feedback loop was tested. The adjustment followed this order. (i) Scan the laser frequency by using the laser servo Ramp signal and look for the  $\text{TEM}_{00}$  mode shown on the camera. Then gradually decrease the scanning range until only the  $\text{TEM}_{00}$  mode appears within one scanning range. (ii) Adjusting the voltage to PZT to find the  $\text{TEM}_{00}$  mode. In order to control the voltage conveniently, one power supply is used in the feedback loop to the PZT. This power supply should have low noise, meanwhile make sure it has fine turning function which makes the adjustment convenient. (iii) When the  $\text{TEM}_{00}$  mode is found, the transmission intensity is very high meanwhile the intensity of the carrier in dispersion curve is higher. (iv) At this moment, the system locking can be tried. Figure 4.11 shows this moment. On the oscilloscope, Channel 1 (white curve) is the transmission intensity and Channel 2 (green curve) is the dispersion curve. The  $\text{TEM}_{00}$  mode pattern is shown on the left monitor. Here one thing should be noticed, on the laser servo front panel there is a ‘gain sign’ switch which changes the sign of the feedback error signal. Switch this sign is equivalent to change the slope polarity of the dispersion curve. Make sure that this switch is at the correct position. Then activate the lock function of the servo, Figure 4.12 shows the signal when the locking is successful.

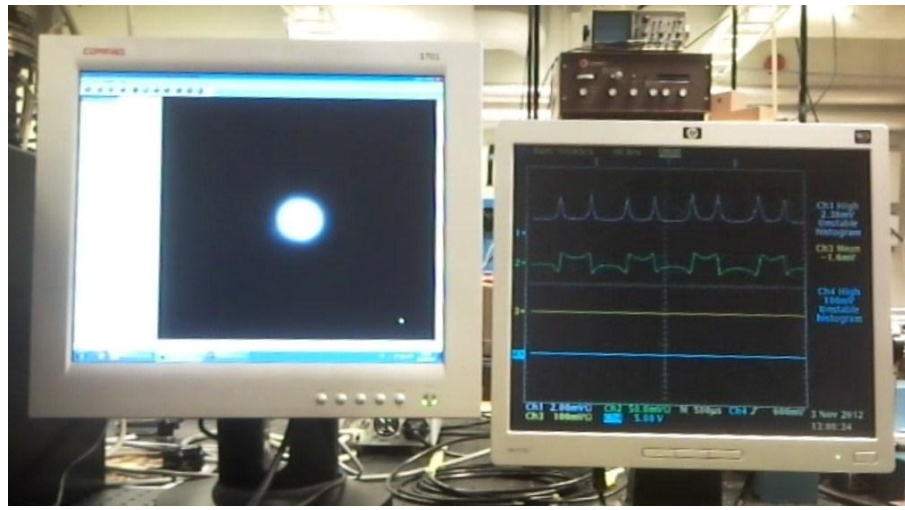


Figure 4.11. The state ready for locking

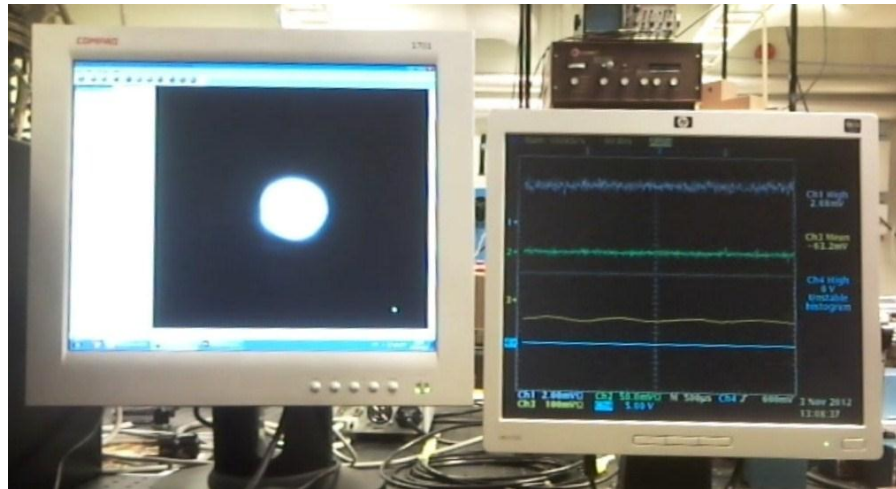


Figure 4.12. The locking state

If the locking can't be succeeded, recheck the slope of the dispersion curve. If the transmission intensity is too low when the system is locked, one could check if the DC offset is still at zero position. This offset should be set around zero level, which will influence the lock point position.

When the current feedback loop is working well, it is time to add the PZT feedback loop into the system. The laser servo has an 'Auxiliary Servo Output' which sends out a voltage regulation signal to the PZT on ECDL trying to keep the laser diode current regulation signal close to zero. This output voltage is in the range of -15 V to 15 V, but the servo voltage to the PZT should be positive, thus a constant voltage should be added to the 'Auxiliary Servo Output'. Here two +9 V batteries are connected in series to protect the PZT. The locking steps are the same as previous. When I tested the stabilization system, the longest locking time was around 2 hours.

#### **4.4 Future work**

The goal of this project is to stabilize the laser frequency at least for 8 hours. Unfortunately the longest lock-in time duration is only ~2 hours. There are still some works to improve, however that is beyond the scope of this thesis due to the time limitation. Here are some suggestions for the future adjustment.

1. The unstable output voltage of the additional power supply will influence the PZT directly, therefore break the locking. Thus, the power supply in the PZT feedback loop should be upgraded.
2. The RF shielding has been mentioned so many times in this report, we think the problem was solved since it can't be detected from the laser intensity, but not sure it disappears completely.

## Acknowledgments

Firstly, I would like to thank Stefan kröll for this opportunity to do my diploma work in quantum information group. I really want to say thank you so much to my supervisor Ying Yan, I have learned too many things about the project and also studied valuable research method. Thanks for your stimulating suggestions, encouragement and patience. I would like to thank my co-supervisor Lars Rippe, you are always full of passion, and all the questions seem to have the answer from you. Your many suggestions help me to solve problems more efficiently.

During the project, there are so many nice memories, such as weekly meeting and lunch, coffee break at 3 PM on time, football golf, challenge activity etc. I would like to thank all the rest group members Jenny, Mahmood and Qian for sharing their experience about the experiment.

Finally, I want to send the best wishes to my parents and sister, for their solicitude and support during this period of study in Sweden.

## Reference

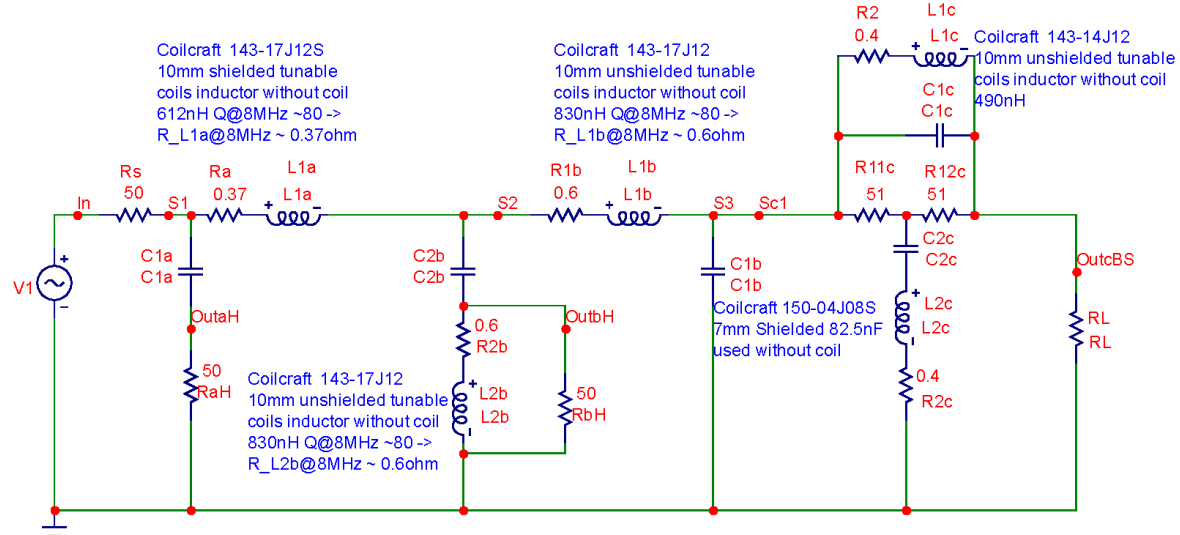
- [1] Eric D. Black, *An introduction to Pound-Drever-Hall laser frequency stabilization*, Am. J. Phys. 69, 79 (2000).
- [2] Samuel Bengtsson, *Simulation and modeling of Rareearth ion based quantum gate operations*, Thesis work, Lund University (2012).
- [3] Wesenberg, J. H., Molmer, K., Rippe, L. & Kröll, S. *Scalable designs for quantum computing with rare-earth-ion-doped crystals*, Phys. Rev.A75,012304 (2007).
- [4] A. Walther, B. Julsgaard, L. Rippe, Y. Ying, S. Kröll, R. Fisher, S. Glaser, *Extracting high fidelity quantum computer hardware from random systems*, Phys. Scr. T137 (2009).
- [5] Johan Tholén, *On the construction of an experimental setup for detection of cerium in Y<sub>2</sub>SiO<sub>5</sub>*, Thesis work, Lund University (2006).
- [6] Cunyun Ye, *Tunable External Cavity Diode Lasers*, word scientific publishing Co. Ltd, 2004.
- [7] A. Walther, *et al.*, *Extracting high fidelity quantum computer hardware from random system*, Phys. Scr. T137, 014009 (2009).
- [8] D2 System DBR Product Manual. Vescent Photonics, Inc. [www.vescentphotonics.com](http://www.vescentphotonics.com)
- [9] ULE Ultra Low Expansion Glass, Specialty Materials. Corning Incorporated. Retrieved 2008.
- [10] J Alnis et. al., *Sub-Hz line width diode lasers by stabilization to vibrationally and thermally compensated ULE Fabry P érot cavities*, Physical Review A 77, 053809 (2008).
- [11] L.Rippe. *Quantum computing with naturally trapped sub-nanometre-spaced ions*. PhD thesis, Division of Atomic Physics, LTH, December 2006.
- [12] Wikipedia. Power supply (2012).  
URL [http://en.wikipedia.org/wiki/Power\\_supply#Linear\\_regulated\\_power\\_supply](http://en.wikipedia.org/wiki/Power_supply#Linear_regulated_power_supply)
- [13] L. Levin, *Mode-hop-free electro-optically tuned diode laser*, Opt. Lett. 27, 237 (2002).
- [14] K.M.Birnbaum, *Ultra-High Vacuum Chambers*, (2005)
- [15] NASA. *Outgassing data for selecting spacecraft materials online*, Technical report, URL <http://outgassing.nasa.gov/>, 2011.
- [16] Laco technology application note, *Vacuum Bake-out of Parts*.
- [17] MDC Vacuum Catalog, *CF Flanges*, section 1.1. URL [www.mdcvacuum.co.uk](http://www.mdcvacuum.co.uk)

- [18] Gamma Vacuum, LLC. Mail communication, 2013.
- [19] Omur Sezerman and Garland Best, *Accurate alignment preserves polarization*, Laser Focus World. 1997
- [20] Practical Uses and Applications of Electro-Optic Modulators. URL  
<http://www.newport.com/store/gencontent.aspx?id=919642&lang=1033&print=1>
- [21] T. Gale, H. Strickner and W. Hayward. Diplexer Supplemental Page (2006). URL  
[http://www.qrp.pops.net/DIP\\_SUP.htm](http://www.qrp.pops.net/DIP_SUP.htm).
- [22] Wikipedia. Microstrip (2012). URL <http://en.wikipedia.org/wiki/Microstrip>
- [23] Wiman Adam, *Laser stabilization to low-expansion fabry-pérot cavity*. Thesis work, Lund University (2011).

# Appendix

## Appendix A

Diplex 1 order 8 MHz LP, 2 order 40 MHz NF, between mixer and integrator



.DEFINE freqa 13MEG

.DEFINE RL 50

.DEFINE C1a 244p

.DEFINE L1a 612n

.DEFINE freqb 13.558MEG

.DEFINE L1b sqrt(2)\*RL/(2\*PI\*freqb)

.DEFINE C1b L1b/(2\*RL^2)

.DEFINE L2b L1b

.DEFINE C2b C1b

    DEFINE L1a RL^2\*C1a     DEFINE C1a 1/(2\*PI\*freqa\*RL)

freqa=13MEG

RL=50

C1a=244p

L1a=612n

freqb=13.558MEG

L1b=830.06n

C1b=166.012p

L2b=830.06n

C2b=166.012p

.DEFINE freqc 40MEG

.DEFINE L1c 490n

.DEFINE C1c 1/(L1c\*(2\*PI\*freqc)^2)

.DEFINE C2c 1/(L2c\*(2\*PI\*freqc)^2)

.DEFINE L2c 82.5n

    DEFINE L1c RL^2\*C2c

freqc=40MEG

L1c=490n

C1c=32.309p

C2c=191.896p

L2c=82.5n

Two stage 8MHz lowpass diplexer filter, followed by a 40MHz notch diplexer filter: Input resistance is 50ohm for all frequencies which means that the reflections will be very low.

All capacitors should be made up from one NPO/COG surface mount capacitor in parallel with suitable variable capacitor to allow adjustment around the given value. Alternatively can just a variable capacitor be used.

With the circuit board specified below the stripes should be 1.85mm wide (for 50ohm impedance). Next to the stripe it should be a 2mm clear to the earth plane.

Interconnections between the top and bottom earth plane should be made on many places.

Rs is the source internal resistance and is not part of the filter. RL is the load resistance and is not part of the filter.

Part of material needed, excluding the components given in the diagram

1p Suitable box(Alubos 1040, the gaskets which have metalparts inside made of silver)

    BOPLA /order from Miltronic

2p Suitable SMA connector

    Circuit board 100\*60mm /order from China(SHENZHEN SEN YAN ELECTRONICS CO., LTD)

C1a: One of each below in parallel

    1p Elfa 65-799-40, 56pF NPO 0805

    1p Farnell 718476, 180pF NPO 0805

    1p Elfa 68-798-03, 2-18pF PTFE film trimmer

RaH: Two of below in parallel

    2p Farnell 9240888 100ohm 1206

Ra: Only for simulation purpose

C1b, C2b: One of each below in parallel

    2p Elfa 65-799-81, 82pF NPO 0805

    2p Elfa 65-799-65, 68pF NPO 0805

    2p Elfa 68-798-03, 2-18pF PTFE film trimmer

R2b: Only for simulation purpose

RbH: Two of below in parallel

    2p Farnell 9240888 100ohm 1206

R2: Only for simulation purpose

C1c: One of each below in parallel

    1p Farnell 756-8568, 22pF NPO 0805

    1p Elfa 68-798-03, 2-18pF PTFE film trimmer

R11c, R12c:

    2p Farnell 933-6656, 51ohm 1206

C2c: One of each below in parallel

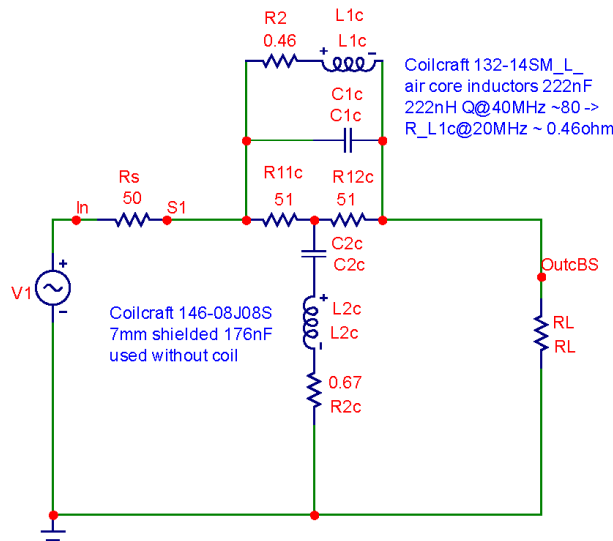
    1p Elfa 65-799-81, 82pF NPO 0805

    1p Farnell 499171, 100pF NPO 0805

    1p Elfa 68-798-03, 2-18pF PTFE film trimmer

R2c: Only for simulation purpose

## Diplex 40 MHz Notch filter, before the phase detector

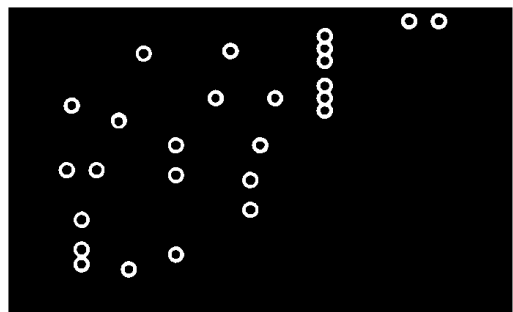
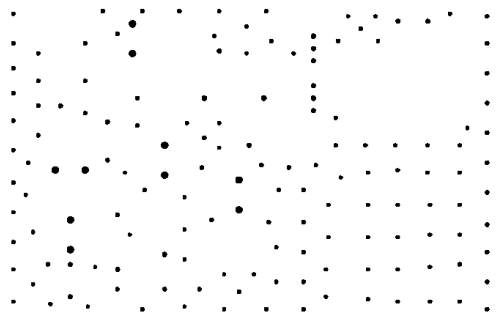


```
.DEFINE freq=40MEG          freqc=40MEG
.DEFINE RL=50                RL=50
.DEFINE L1c=222n              L1c=222n
.DEFINE C1c=70p               C1c=70p
.DEFINE C2c=88p               C2c=88p
.DEFINE L2c=176n              L2c=176n
```

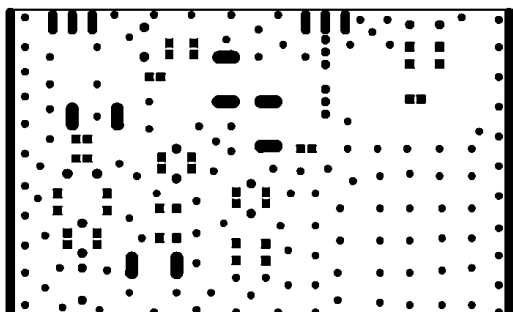
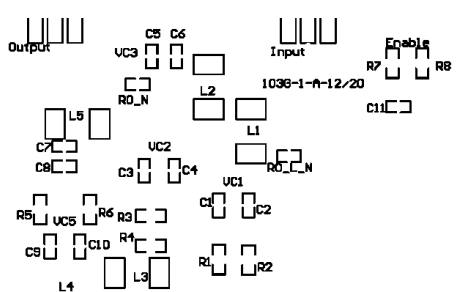
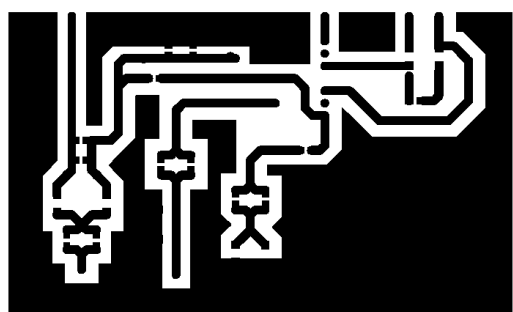
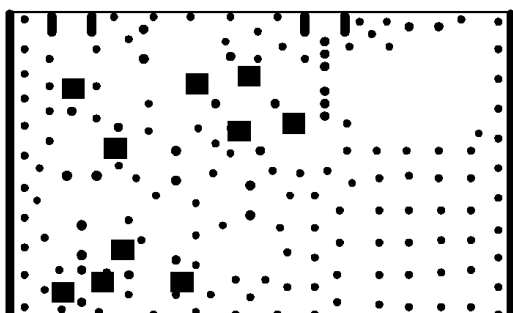
DEFINE L1c RL^2\*C2c

40MHz notch diplexer filter: Input resistance is 50ohm for all frequencies which means that the reflections will be very low.  
All capacitors should be made up from one NPO/COG surface mount capacitor in parallel with suitable variable capacitor to allow adjustment around the given value. Alternatively can just a variable capacitor be used.  
With the circuit board specified below the stripes should be 1.85mm wide (for 50ohm impedance). Next to the stripe it should be a 2mm clear to the earth plane.  
Interconnections between the top and bottom earth plane should be made on many places.  
Rs is the source internal resistance and is not part of the filter. RL is the load resistance and is not part of the filter.

Part of material needed, excluding the components given in the diagram  
1p Suitable box(Alubox 1040, the gaskets which have metalparts inside made of silver)  
BOPLA /order from Miltronic  
2p Suitable SMA connector  
Circuit board 100\*60mm order from China(SHENZHEN SEN YAN ELECTRONICS CO., LTD)  
R2: Only for simulation purpose  
C1C: One of each below in parallel  
1p Elfa 65-799-40, 56pF NPO 0805  
1p Elfa 68-798-03, 2-18pF PTFE film trimmer  
R11c,R12c:  
2p Farnell 933-6656, 51ohm 1206  
C2c: One of each below in parallel  
1p Elfa 65-799-81, 82pF NPO 0805  
1p Elfa 68-798-03, 2-18pF PTFE film trimmer  
R2c: Only for simulation purpose



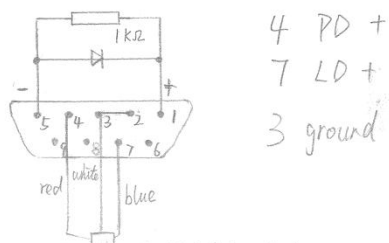
White Top Pass  
8 Dots Per Pixel  
Filter Top Edge  
Raster Leadership Separation System



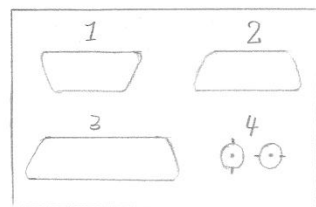
## Appendix B

### ECDL Back Panel Connection Situation

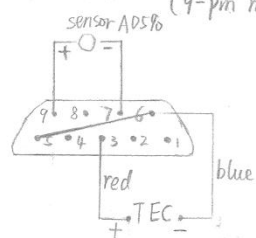
#### I. Laser diode (9-pin female)



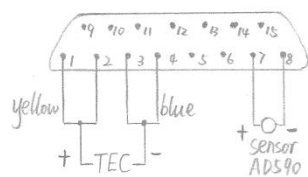
Back panel



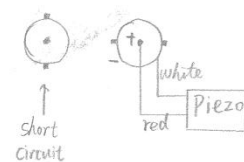
#### 2. Laser diode temperature (9-pin male)



#### 3. Monolith temperature (15-pin female)



#### 4. crystal voltage (BNC)

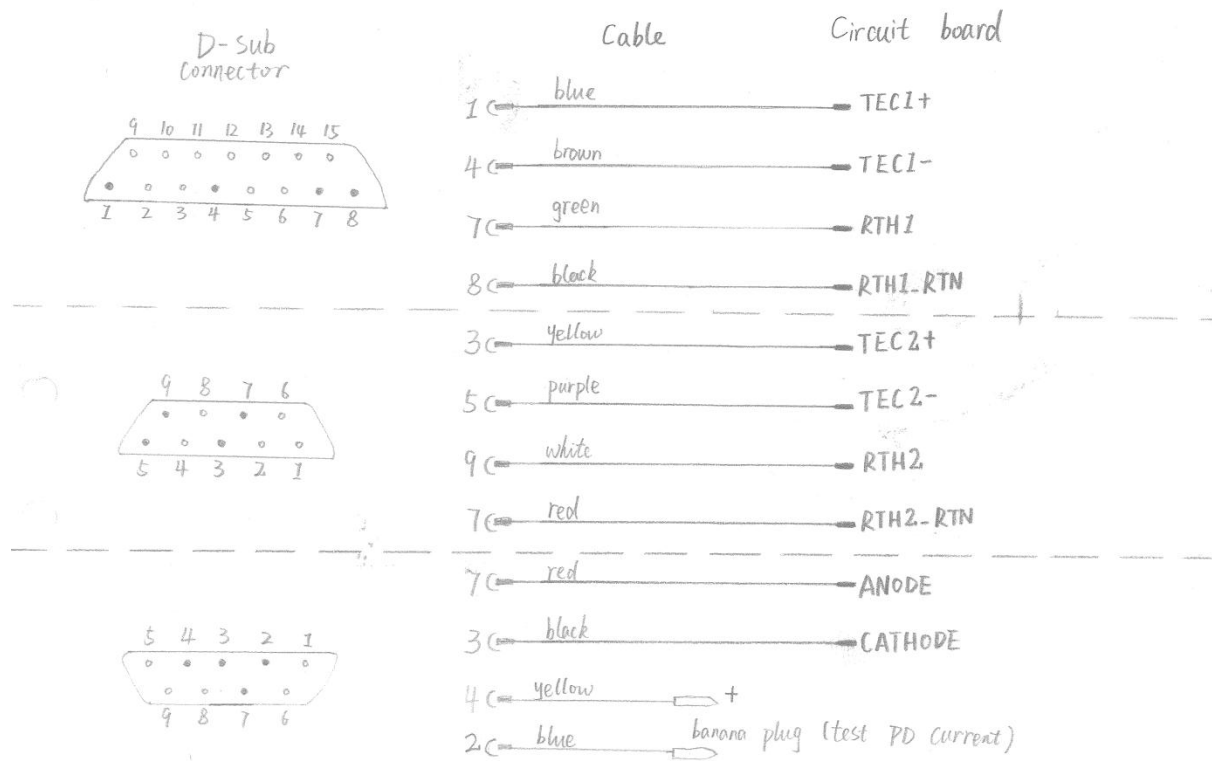


In order to connect the ECDL with the new laser controller, the new connection method is recorded below.

A simple circuit board has been used.

3 ①	• TEC1+	8-Pin Hirose connector
3 ④	• TEC1-	
3 ⑦	• RTH1	
3 ⑧	• RTH1_RTN	
2 ③	• TEC2+	
2 ⑤	• TEC2-	
2 ⑨	• RTH2	
2 ⑩	• RTH2_RTN	
1 ⑦	• ANODE	SMA connector
1 ③	• CATHODE	
	VPN00187.2	Vescent Photonics

The circuit board connection situation (VPN00187.2 Vescent Photonics)



## Appendix C

The baking out recording (Unit Temperature: °C      Pressure: mbar)

### The first baking out

Date	Time	Temp.1 Valve body	Temp. 2 View port 1	Temp. 3 Chamber body	Temp. 4 View port 2	Heater	Turbo pump pressure	Ion pump pressure
05.04	11:06						6.3	
	11:18						8.6e-5	
	13:15						4.6e-6	
	15:25						1.6e-6	
	17:02						1.2e-6	
	18:37	27	26	27	26	5	1.6e-6	
	19:30	35	31	35	30	10	1.6e-6	
05.05	09:15	45	39	43	37	10	6.3e-7	
	10:50	67	51	62	49	18	1.2e-6	
	13:30	91	68	80	64	20	2.5e-6	
	16:40	67	57	61	54	11	7.4e-7	
05.07	08:30	42	36	40	35	10	5.4e-7	
	10:40	66	50	60	47	18	8.6e-7	
	16:48	103	78	90	71	22.5	7.4e-7	
	18:41	100	77	87	71	20	7.4e-7	
05.08	09:40	93	71	86	64	25	6.3e-7	
	13:00	115	86	104	77	26	7.4e-7	
	17:00	107	83	98	76	25	5.4e-7	
	19:35	103	81	94	73	23	6.3e-7	
05.09	09:25	99	76	90	68	24	4.0e-7	
	11:53	111	84	102	76	27	4.6e-7	
	14:40	114	87	105	79	27	6.3e-7	
	20:16	101	80	94	73	23	5.4e-7	
05.10	08:30	95	74	88	67	23	3.4e-7	
	13:15	117	89	108	80	26	7.4e-7	
	18:30	111	86	103	78	24	4.6e-7	
	20:30	102	81	95	73	24	5.4e-7	
05.11	09:50	101	78	93	69	25	5.4e-7	
	11:10	109	82	100	74	26	4.6e-7	
	13:26	116	88	106	80	26.5	5.4e-7	
	17:50	113	87	104	79	24	5.4e-7	
05.13	13:30	100	77	92	69	24	5.4e-7	
05.14	08:45	99	76	91	69	24	3.4e-7	
	10:40	81	66	76	61	19	3.4e-7	
	15:02	48	45	47	43	6	3.0e-7	
	18:06	30	29	31	30	0	3.4e-7	

## The second baking out (The ion pump has been installed)

Date	Time	Temp.1 Valve body	Temp. 2 View port 1	Temp. 3 Chamber body	Temp. 4 View port 2	Heater	Turbo pump pressure	Ion pump pressure
05-15	13:00						room	
	13:07						8.6e-5	
	13:55						1.0e-5	
	14:30	25	24	25	24	5	4.0e-6	
	15:30	25	27	35	29	14	1.9e-6	
	16:35	25	37	55	42	18	1.2e-6	
	17:35	25	46	69	52	20	1.0e-6	
	18:40	78	55	82	62	24	8.6e-7	
	20:50	98	68	101	77	24	6.3e-7	
05-16	09:20	108	75	109	84	24	7.4e-7	
	10:25	100	72	100	80	20	4.6e-7	
	12:10	76	59	75	64	12	4.0e-7	
	14:30	48	42	48	44	2	4.0e-7	
	15:30	38	36	39	36	0	7.4e-7	

Turn on the ion pump when the temperature decreases to normal. The valve of the turbo pump should not be closed tight.

	18:15	25	25	25	25	0	stop	3.0e-6
	20:00							1.6e-6
05-17	11:00							5.05e-8
	16:00							9.6e-8
	20:20							4.6e-8
05-18	09:20							3.8e-8

The screws were fixed again

	10:50							4.3e-8
	14:00							2.9e-8
	16:00							1.0e-6

Turn on the turbo pump

05-21	08:30						5.0e-7	
	10:25						stop	5.4e-6
	10:30							2.6e-6
	14:15							3.6e-6
05-22	08:35							5.09e-8
	10:35							7.8e-8
	18:20							6e-8
05-23	08:40							5.1e-8
	18:40							6.2e-8
05-24	08:40							5e-8
05-25	09:10							5.22e-8
	17:15							5.8e-8
05-28	09:40							7.75e-8

## Baking the radiation shield

Date	Time	Temp. 1 Valve body	Temp. 2 View port 1	Temp. 3 Chamber body	Temp. 4 View port 2	Heater	Turbo pump pressure	Ion pump pressure
05-30	21:00						3.5e-5	
05-31	08:40	22	22	21	22	0	1.6e-6	
	10:40	23	23	24	23	10	1.2e-6	
	13:10	49	50	75	54	21	5.4e-6	
	16:20	61	56	78	65	18	7.4e-6	
	20:05	61	57	78	67	18	3.4e-6	
06-01	08:35	60	56	77	66	18	1.0e-6	
	13:30	71	64	91	76	21	1.4e-6	
	14:45	76	68	99	80	23	1.6e-6	
	16:45	68	63	85	76	17	1.4e-6	
	18:05	52	52	59	61	6	8.7e-7	
	18:31	48	48	55	56	6	7.4e-7	
	19:45	50	48	64	54	15	8.6e-7	
	20:45	59	55	80	61	20	7.4e-7	
06-03	15:30	68	63	90	73	20	5.4e-7	
06-04	09:40	67	62	89	73	20	4.6e-7	
	10:45	63	59	82	70	14	4.6e-7	
	12:30	46	46	53	54	3	4.6e-7	

## Turn on the ion pump

## Baking out after the cavity spacer installation

Date	Time	Temp.1 Inside cavity	Temp. 2 View port 1	Temp. 3 Chamber body	Temp. 4 View port 2	Heater	Turbo pump pressure	Ion pump pressure
06-30	01:30	26.5	25	30	25	10	1.6e-4	
	15:00	30.5	28	33	28	15	3.0e-6	
	16:30	35	31	43	31	19	3.0e-6	
	18:00	40	35	51	35	18	3.4e-6	
07-02	09:00	45	38	52	37	18	7.4e-7	
	18:00	45	40	54	40	18	7.4e-7	
07-03	09:05	47	38	53	38	18	5.4e-7	
	18:00	47	38	53	38	18	5.4e-7	
07-04	08:50	47	38	53	38	18	4.6e-7	
<b>Turn on the ion pump</b>								
	11:20	47	38	53	38	18	4.6e-7	7.75e-6
<b>Turn off the ion pump and the heater.</b>								
	11:53		38	49	39	12	4.6e-7	
	14:30		30	30	31	0	4.0e-7	
<b>Turn on the ion pump</b>								
	16:20		27	27	27	0	5.4e-7	3.9e-6
	16:27		27	27	27	0	Off valve	8.0e-6
	18:50		25	26	26			2.76e-6
07-05	08:50							1.64e-6
	12:15							1.62e-6
	16:00							1.48e-6
	18:40							1.33e-6
07-06	08:38							1.09e-6
	11:50							1.19e-6
	18:30							1.38e-6
	20:20							1.52e-6
07-09	07:45							2.36e-6
	10:35							1.81e-6
07-10	08:40							1.99e-6
<b>Check with the turbo pump and try to decrease the pressure</b>								
	11:35						Open valve fully	stop
	11:35						8.6e-7	
	12:26	24.5	23	23	23	10	7.4e-7	
	14:23	16.52k	29	42	28	18	5.4e-7	
	18:45	7.2k	45	61	43	20	6.3e-7	
07-11	08:40	50	43	59	42	20	5.4e-7	
	11:00	5.3k	51	80	49	26	5.4e-7	
	15:10	4.0k	57	89	55	29.5	7.4e-7	
	18:43	2.65k	65	105	63	32	1.0e-6	
	20:50	76	64	97	62	25	8.6e-7	
	21:50	3.44k	58	82	56	23	7.4e-7	
	22:25	65	54	73	53	19	6.3e-7	

Date	Time	Temp.1 Inside cavity	Temp. 2 View port 1	Temp. 3 Chamber body	Temp. 4 View port 2	Heater	Turbo pump pressure	Ion pump pressure
07-12	09:10	7.44k	43	60	42	19	4.0e-7	
	11:00	5.87k	49	79	47	27	4.0e-7	
	13:45	72	64	105	60	33	5.4e-7	
	16:00	80	69	110	65	33	7.4e-7	
	18:15	2.26k	71	112	67	33	8.6e-7	
	19:30	2.27k	70	107	66	27	7.4e-7	
	20:35	74	62	80	60	18	5.4e-7	
07-13	09:30	8.45k	41	55	40	18	4.0e-7	
	11:50	39	34	38	32	5	3.4e-7	
	14:10	28	26	25	25	0	3.4e-7	

**Turn on the ion pump**

	15:05	18.52k	24	24	23	0	5.4e-7	6.0e-6
	15:40	19.18k	24	23	23	0	Off valve	2.8e-6
	16:30	19.80k	23	23	23	0		1.0e-6
07-15	21:15							3.6e-7
07-16	08:45							3.42e-7
	19:30							4.3e-7
07-17	09:35							4.2e-7
	22:00							3.1e-7
07-18	08:40							4.0e-7
07-19	13:00							3.6e-7
07-20	09:30							2.8e-7
07-23	09:00							2.17e-7
07-24	11:30							2.16e-7